Impacts of microplastics exposure on mussel (*Mytilus edulis*) gut microbiota

Luen-Luen LI[1,2], Rachid AMARA[1], Sami SOUISSI[3], Alexandre DEHAUT[2], Guillaume DUFLOS[2], Sébastien MONCHY[1*]

[1] Univ. Littoral Côte d'Opale, CNRS, Univ. Lille, UMR 8187, LOG, Laboratoire d'Océanologie et de Géosciences, F 62930 Wimereux, France

[2] ANSES, Laboratoire de Sécurité des Aliments, Boulevard du Bassin Napoléon, 62200, Boulogne-sur-mer, France

[3] Univ. Lille, CNRS, Univ. Littoral Côte d'Opale, UMR 8187 - LOG - Laboratoire d'Océanologie et de Géosciences, F-59000 Lille, France

* Corresponding author

Corresponding author email address: Sebastien.Monchy@univ-littoral.fr

Corresponding author post address: Laboratoire d'Océanologie et de Géosciences, 32 av. Foch, 62930 Wimereux, France

Hightlights

- Microplastics ingestion altered gut microbiota of the filter feeder - blue mussels.
- Biofouled/weathered & high concentration MPs had greater impacts on microbiota.
- Potential human pathogens were among taxa with higher abundance after MP-exposure.
- Feces of MP-exposed mussels may influence microbiota of surrounding environment.

Abstract

Microplastics (MPs), plastics with particles smaller than 5 mm, have been found almost in every corner of the world, especially in the ocean. Due to the small size, MPs can be ingested by animals and enter the marine trophic chain. MPs can affect animal health by physically causing damage to the digestive tract, leaking plastic chemical components, and carrying environmental pollutants and pathogens into animals. In this study, impacts of MPs ingestion on gut microbiota were investigated. Filter feeding mussels were exposed to "virgin" and "weathered" MPs at relatively realistic concentration 0.2 mg L^{-1} ('low") and exaggerated concentration 20 mg L^{-1} ('high") for 6 weeks. Influence in mussel gut microbiota was investigated with 16S rRNA gene high-throughput sequencing. As compared with non-exposed mussels, alteration of gut microbiota was observed after mussels were exposed to MPs for 1 week, 3 weeks, 6 weeks, and even after 8-day post-exposure depuration. Potential human pathogens were found among operational taxonomic units (OTUs) with increased abundance induced by MP-exposure. Fecal pellets containing microorganisms from altered gut microbiota and MPs might further influence microbiota of surrounding environment. Our results have demonstrated impacts of MP-exposure on mussel gut microbiota and suggested possible consequent effects on food quality, food safety, and the well-being of marine food web in the ecosystem for future studies.

Keywords

Microplastics, Microbiota, Blue mussels, High-throughput sequencing, bioinformatics, food safety

1. INTRODUCTION

Plastics pollution has become an emerging global concern as most of plastics waste end up in the world's oceans [1, 2]. In 2017, the amount of plastic waste entering the oceans each year from land-based sources was estimated at 8.75 million metric tons [3, 4]. In addition, more than half a million metric tons of "ghost gear" get lost in the sea by the fishing industry every year and most of which is plastic [5]. Plastics debris in the sea are subject to mechanical abrasion, photo-degradation, oxidation, and biological fouling. Consequently, plastics debris may be broken down into small fragments and become microplastics or even nanoplastics [6]. Microplastics (MPs) can also come from direct industrial productions (e.g. microbeads for cosmetics) and synthetic fibers released from our laundry [7]. So far, microplastics have been found in every corner where surveys were conducted, including remote islands [8], polar ice [9, 10], and the deep sea [11, 12]. Under environmental forces such as turbulence, ultraviolet radiation, and salinity, surface properties of MPs (roughness, charge, hydrophobicity, polarity, etc.) would be affected [13]. Such surface features could make MPs attract not only pollutants like persistent organic pollutants (POPs) and heavy metals, but also microorganisms to form biofilms and plastisphere [14].

Previous studies have shown that, due to their small size (< 5mm), MPs can be ingested by marine animals such as zooplankton, polychaetes, fish, and bivalves [15-18]. MPs can also be ingested directly or indirectly by animals of higher trophic levels, such as seals, dolphin, and even whale [19, 20]. Besides accumulation in the digestive tract [16-18, 21], MPs also may be translocated to other tissues/organs such as the circulatory system and liver [22, 23], and adhere to gills or soft tissues [24]. Internalized MPs can physically cause damage to the digestive tract [25] and chemically leak plastic components such as bisphenol A and plasticizers [26]. Moreover, environmental pollutants and microorganisms/pathogens may use MPs as a vector to get into animals and cause harm [27]. Lately, studies start to reveal effects of

MPs on animal health, for instance, feeding behavior changes [28, 29], growth or development alteration [30, 31], reduced efficiency in food assimilation [32], impacts on reproduction [28, 33], and oxidative stress or damage [34, 35]. However, mechanisms that cause these effects are not yet clear and need further investigation.

In recent years, attention has been brought to the importance of microbiota. The microbiota affects host physiology and health to a great extent [36]. Reciprocally, intrinsic host traits and environmental factors also shape microbiota of the host [37]. It has been shown that a balanced and healthy gut microbiome can serve as a buffer to prevent infection and support the host immune system [38, 39]. Nevertheless, substantial alteration in gut microbial community composition and abundance can cause functional dysbiosis, thus leading to changes in susceptibility to pathogenic infections and development of diseases [40, 41]. Altogether, it is reasonable to suspect that ingestion of MPs, especially seawater-aged MPs with biofouling/biofilms, could influence microbiota, induce dysbiosis, and consequently affect animal health.

A number of reports have demonstrated the ingestion of MPs by mussels and emerging physiological effects [16, 24, 31, 42-56]. Thus far, only a handful of studies have investigated effects of MPs on gut microbiota, and mostly with model animal zebrafish and mice [34, 57-62]. In this study, marine bivalve blue mussel (*Mytilus edulis*) was selected as the subject of experiments for investigating influence of MPs exposure on gut microbiota. Mussels are one of the major seafood harvested both from the wild and by farming. Due to their commercial value and the fact that the whole organism inside the shell including gut is consumed by human, MPs contaminations of bivalves became a great concern for food safety and human health [63]. Besides to be served as food, mussels also play an important role in aquatic ecosystems [64]. As filter feeders, mussels accumulate pollutants and particles from surrounding waters including heavy metals, pathogens, and MPs, thus are commonly used as sentinel organisms or bioindicators to monitor pollution in coastal environments [65-68]. However, to our knowledge,

correlation between MPs ingestion and influences on mussel gut microbiota has not yet been investigated. Therefore, we hypothesize that MPs ingestion could alter mussel gut microbiota.

In the present study, impacts of MPs exposure on mussel gut microbiota were investigated. Blue mussels were exposed to two types of HDPE MPs: pristine condition (labeled as “virgin” MPs in this manuscript) and seawater treated/biofouled (labeled as “weathered” MPs). For each type of MPs, two concentrations were tested: "Realistic" and "High" (see details in material and methods). The duration of MPs exposure was six weeks and community compositions of mussel gut microbiota were accessed by performing 16S rRNA amplicon high-throughput sequencing.

2. MATERIAL AND METHODS

2.1 Biological material - Mussel collection

Blue mussels (*Mytilus edulis*) (length 49.5 ± 2.5 mm; width 23.4 ± 1.3 mm; height 16.3 ± 1.5 mm) were obtained from a commercial farm (50°52'28.2"N 1°36'40.3"E, Cap Gris-Nez, France). All mussels were immediately transported to the laboratory and scrubbed to remove epibionts/fouling organisms from valves before the acclimation process.

2.2 Chemical material – Microplastics

Two types of high-density polyethylene (HDPE) microplastics, with mean particle-size 4–6 µm (reference MPP-635XF) and 20–25 µm (reference MPP-1241), were obtained from Micro Powders Inc. (Tarrytown, NY, USA). According to the manufacturer, the density at 25 °C of this HDPE is 0.96 g/cm^3. In this study, equal amount (mass) of the two MPs were prepared into a mixture for each individual exposure experiment. Two concentrations of MPs were tested: “Realistic” - 0.2 mg L^{-1} (~1,170 MPs mL^{-1}), a concentration that is considered as realistic concluding from results of available surveys, mostly with manta trawl sampling method (labeled as "low" in this manuscript)[69] and “High” - 20 mg L^{-1} (~117,000

MPs mL^{-1}) that is one hundred fold of the “realistic” concentration (labeled as "high") [69, 70]. In order to test effects of MPs closer to environmental conditions, besides MPs in the pristine condition (“virgin” MPs), seawater treated MPs (“weathered” MPs) were also prepared. Briefly, MPs were mixed with 20 µm filtered natural seawater (to exclude zooplankton and most microplankton) in individual 100 mL sterilized glass bottles and incubated at room temperature on a rotary shaker (at 150 rpm) for one month before being applied into mussel cultures for MPs exposure experiments. Microbial community composition on "virgin" and "weathered" MPs were as well analyzed in this study.

2.3 Mussel culture conditions

Culture experiments were conducted at the climate controlled facility of Laboratoire d’Océanologie et de Géosciences (LOG CNRS UMR 8187, Wimereux, France) with temperature at 12.5 ± 0.5 °C and a 10-hour/14-hour Light/dark cycle. These parameters are consistent with environmental conditions occurring at the mussel farm. Before experiment, all glassware was cleaned with detergent, 5% HCl (acid-washed), thoroughly rinsed and soaked with deionized water, soaked overnight in filtered (1µm) seawater, and rinsed again with filtered seawater. Mussels were cultivated in glass aquaria tanks with natural seawater successively filtered at 100µm, 50µm, 25µm, 10µm and finally 1µm with continuously air supply. Seawater conditions were as follow: pressure: 757.2 ± 6.2 mmHg; salinity: 32.2 ± 2.3 ; O_2: 98.5 ± 1.5 %; pH: 7.6 ± 0.4. During the period of experiment, every tank was cleaned and seawater was renewed three times per week. Aquariums were covered with glass plate in order to avoid loss of MPs and contamination with external particles. To prevent MPs leak from the laboratory, all wastewater was filtered with 1 µm NITEX filter (Sefar NITEX 03-1/1, Sefar AG, Heiden, Switzerland) before discharges. After water change, mussels were fed with a mixture of pure cultured microalgae *Tisochrysis lutea* and *Rhodomonas marina* (around 10^6 cells of *Rhodomonas* and 10^7 cells of *Tisochrysis* per mussel per feeding) produced continuously in the laboratory using standard protocols [71].

2.4 Microplastics exposure experiments

The acclimation process was carried out in two 250-L glass tanks (duplicate) for 7 days. At the beginning and the end of the acclimation, 4 mussels from each tank were sampled for microbiota analysis and 5 mussels for physical conditions (shell size and dry meat weight) monitoring. Immediately after the acclimation, MPs exposure experiments were started. The exposure and post-exposure depuration were carried out in ten 35-L glass tanks, with 40 mussels per tank. The mussel MPs exposure experiment consist of five conditions: (1) Control - without MPs; (2) "Virgin" MPs – low concentration ; (3) "Virgin" MPs – high concentration ; (4) "Weathered" MPs – low concentration; (5) "Weathered" MPs – high concentration, each condition in duplicate. The duration of the MPs exposure experiment was 6 weeks; therefore, the mussel gut microbiota could have time to reach a homeostasis. Three times per week, every tank was cleaned and seawater was renewed, followed by microalgae feeding and MPs exposure with above-mentioned five conditions. Microplastics for each exposure tank were prepared in individual 100 mL sterilized glass bottles, mixed with 1µm filtered seawater, then poured into the tank. After 6 weeks MPs exposure, an 8-day post-exposure depuration process was performed with the same incubation and feeding routines but excluded MPs exposure. The mussels were sampled after 1-week, 3-week, and 6-week exposure, as well as after 2-day and 8-day post-exposure depuration. The reason for sampling after 2-day depuration is because in many countries, depuration of bivalves is mandatory around 48 hours before retail sale [72]. At each sampling time, 7 mussels (4 for microbiota analysis and 3 for condition index monitoring) were randomly selected from each tank. Mussel feces/tank water microbiota samples (tank water contents including feces, pseudofeces and other waste from mussels, to simplify, "feces/tank water microbiota" was used in this manuscript) from every culture tank was also collected by filtering seawater through the Sterivex filter unit (Millipore, Burlington, MA, USA). Mussels were opened, thoroughly rinsed with sterilized MilliQ water, and intestines were immediately extracted by dissecting individual mussel with sterilized surgical scalpels and tweezers, and then stored at -20°C prior to microbiota DNA extraction.

2.5 Microbiota DNA extraction, 16S rRNA gene library preparation, and next generation sequencing

To extract mussel gut microbiota DNA, two mussel intestines were pooled together, homogenized, and total DNA was extracted by using the Allprep PowerFecal DNA/RNA Kit (Qiagen, Hilden, Germany) following the manufacturer's instruction. The concentration and quality of extracted DNA were checked by using the Qubit Fluorometer (Thermo Fisher Scientific, Waltham, MA, USA). The 16S amplicon library was prepared according to a standardized protocol (Metabiote®, GenoScreen, Lille, France). Briefly, the V3-V4 region of bacterial 16S ribosomal RNA gene was amplified by using universal primers 341F (5'-CCTACGGGNGGCWGCAG -3') and 805R (5'- GACTACHVGGGTATCTAATCC -3') tagged with 28 bp overhang adapters. The Invitrogen Platinum SuperFi DNA Polymerase (Thermo Fisher Scientific, Waltham, MA, USA) was utilized for PCR reactions according to the manufacturer's instruction. All PCR products were examined on 1% agarose gel electrophoresis and then purified with the Agencourt AMPure XP PCR purification system (Beckman Coulter, Brea, CA, USA). Following, secondary PCR reactions (index PCR) were performed in order to add Illumina sequencing indices and adapters. After purification with the Agencourt AMPure XP system, quality of 16S libraries were checked using the Quant-iT PicoGreen Assay (Thermo Fisher Scientific, Waltham, MA, USA) and the Agilent Bioanalyzer 2100 system (Agilent Technologies, Santa Clara, CA, USA). 16S amplicon libraries were multiplexed at equal concentrations and the Illumina MiSeq paired-end sequencing (Illumina, San Diego, CA, USA) was performed at the sequencing facility of GenoScreen (Lille, France). Sequencing data have been submitted to the NCBI sequence read archive database (SRA accession: PRJNA612500).

2.6 Sequences processing

The rDNA sequences were processed with the MOTHUR program v1.42.0 [73] following the standard operating procedure (http://www.mothur.org/wiki/MiSeq_SOP) [74]. Sequences were extracted and separated according to their index tag, de-replicated to unique sequence and aligned against the SILVA

184 database (http://www.arb-silva.de/) [75]. Suspected chimeras were eliminated by using the UCHIME
185 software [76]. After quality filtering, an average of 28,853 reads per sample were clustered into
186 operational taxonomical units (OTUs) at 97% similarity threshold [77], using the average neighbor
187 method in Mothur. Single singleton, referring to OTU that has a single representative sequence in the
188 whole data set, were removed as these are most likely erroneous sequencing products [77, 78]. After
189 normalization of the entire dataset, all remaining 6,504 OTUs sequences were searched against the
190 SILVA database (Release 132) [75] by using BLASTN [79]. BLASTN results were carefully examined and
191 manually curated to assign putative taxonomic affiliations for each OTU.

192 **2.7 Bioinformatics and statistical analyses**

193 Alpha diversity estimators (the richness estimator Chao-1, Simpson, Shannon, and Equitability indices)
194 were calculated using the Past 3.26 software [80] for all samples. Comparison of alpha diversity
195 estimators between conditions were evaluated with repeated-measures analysis of variance (ANOVA)
196 and linear mixed-effects model using R software (v 3.6.1) with the "nlme" package [81]. Microbial
197 assemblages (based on OTUs) were grouped across samples by hierarchical cluster analysis using the
198 PRIMER version 6.1.9 [82] based on Bray-Curtis dissimilarity coefficients calculated with double square
199 root OTUs reads abundance normalization. Similarity profile test (SIMPROF) was also performed using
200 the Primer 6 software [82] to define significant similar clusters. The dispersion of different groups was
201 visualized by non-metric multidimensional scaling (NMDS) and permutational analysis of variance
202 (PERMANOVA) was calculated to compare the significant (p-value < 0.05) differences of gut microbial
203 community structure between different treatments and over time. Both analyses were performed using
204 R software with the "vegan" package [83].
205 For samples that were collected at the same time point, by individual OTU, read counts difference
206 between the control and treatment conditions were determined using non-parametric Wilcoxon test
207 using the R software with the "vegan" package and a p-value < 0.05 was considered significantly

different. In addition, differences regarding the relative abundance of operational taxonomic units between the control and MPs-exposed mussels were further determined using the linear discriminant analysis effect size (LEfSe) program [84]. LEfSe is a biomarker discovery and explanation tool for high-dimensional data. It couples statistical significance with biological consistency and effect size estimation. Default input parameters of LEfSe were as follows: the alpha value for the factorial Kruskal-Wallis sum-rank test was 0.05 and the threshold on the logarithmic linear discriminant analysis (LDA) score for discriminative features was 2.0 [84]. The LefSe analysis was complemented by indicator analysis performed using R software with the "indicspecies" package [85].

Finally, the functional profile of microbial community was predicted for each condition using “the phylogenetic investigation of communities by reconstruction of unobserved states” (PICRUSt) program [86] based on phylogenetic information. The OTUs with significant difference in relative abundant between conditions (Mann-Whitney test) were used to infer difference in metabolic pathways among condition. The obtained hierarchical data were collapsed to a specified level for functional predictions, and genes in Kyoto Encyclopedia of Genes and Genomes (KEGG) orthologs database were used to generate pathway counts by sample.

3. RESULTS

3.1 Measurements of mussels condition indices

Throughout the entire experimental period, no significant differences in shell size measurements or in dry meat/dry shell weight ratio between the control and the MPs exposure groups was observed.

3.2 16S rRNA sequence analysis

A total of 6,504 OTUs were identified (exclude single singleton) from 127 16S rRNA libraries (104 gut microbiota, 20 feces/tank water microbiota, and microbial communities on "virgin" and "weathered" MPs, microbiota of filtered seawater supply for mussel culture tanks). Overall, throughout the different

232 stages of the experiment, the microbial diversity per sample for gut microbiota was composed of 1,074 ±
233 115 OTUs before the acclimation, 239 ± 14 OTUs after the acclimation, 227 ± 37 OTUs within the MPs
234 exposure period, 220 ± 52 OTUs within the post-depuration period, and 483 ± 79 OTUs for feces/tank
235 water microbiota. In addition, 781 OTUs were identified from the filtered seawater, 15 OTUs on the
236 "virgin" MPs, and 277 OTUs on one-month "weathered" MPs libraries. Generally, samples could be
237 categorized into three groups: input microbiota (filtered seawater, virgin MPs, and weathered MPs) –
238 977 OTUs, mussel gut microbiota – 3,705 OTUs, and output microbiota (feces/tank water) – 2,766 OTUs.
239 As showed in Fig. 1a, input microbiota and mussel gut microbiota have 405 OTUs in common; input
240 microbiota and output microbiota have 345 OTUs in common; mussel gut microbiota and output
241 microbiota have 1,541 OTUs in common; all three groups of microbiota have 266 OTUs in common.
242 Further focusing on MPs and gut microbiota, 73% of OTUs in "virgin" MPs microbial community and 30%
243 of OTUs in "weathered" MPs microbial community were also found in mussel gut microbiota (Fig. 1b).
244 Alpha diversity for gut microbiota revealed that Equitability (Simpson and Shannon) and dominance
245 (Berger-Parker) estimators (Supplementary material 1) were significantly influenced by exposure time (*p*-
246 value < 0.01). While interaction of MP type and concentration had an effect on Shannon index (*p*-value =
247 0.04672), Berger-Parker index was significantly influenced by interaction of MP type and exposure time
248 (*p*-value = 0.0351). However, when performing repeated-measures analysis of variance (ANOVA) and
249 linear mixed-effects model, grouped by exposure time, no difference was observed in alpha diversity and
250 relative abundance of dominant taxa according to the treatment applied.
251 Hierarchical cluster analysis, based on Bray-Curtis dissimilarity, has shown that samples were clustered
252 according to their origin (Fig. 2 and Supplementary material 2). Indeed, gut microbiota, feces/tank water
253 microbiota, MPs-associated microbiota, and filtered seawater microbiota were clustered separately. In
254 addition, within gut and feces/tank water microbiota clusters, samples were generally first grouped by
255 replicates and then by exposure time (e.g. 1, 3 and 6 weeks exposure) (Fig. 2 and Supplementary

material 2). Interestingly, within sub-cluster of 1-week, 3-week, and 6-week, non-exposed control samples and "weathered-high MPs"-exposed samples were always in distantly different clusters. Additionally, non-exposed samples were often grouped with "virgin-low MPs"-exposed samples, and "weathered-low MPs"-exposed samples were often grouped either with "virgin-high MPs"-exposed samples or with "weathered-high MPs"-exposed samples. Regarding the post-exposure depuration, gut microbiota samples displayed similar clustering as above after two days depuration. However, no particular clustering trend could be observed after eight days depuration. It should be noted that microbiota of one-month "weathered" MPs clustered together with microbiota of seawater that was used for weathering the MPs. Finally, non-metric multidimensional scaling (nMDS) plot, based on Bray-Curtis dissimilarity, was carried out to visualize the dispersion of different groups during the MPs exposure and depuration (Fig. 3). Interestingly, permutational analysis of variance (PERMANOVA) (Table 1) revealed that exposure time (p-value < 0.01), type ("virgin" or "weathered") of MPs (p-value < 0.02), as well as the interaction of factors "MP-type + time" (p-value < 0.01) and "MP-type + concentration" (p-value < 0.05) significantly influenced gut microbiota during the 6 weeks exposure period. Considering the effect of MPs exposure overtime, it appears that the gut microbiota community structure was significantly influenced (p-value < 0.05) by the type of MPs ("virgin" or "weathered") during Week 1, 6, and the initial phase of the depuration (after 2-day depuration), and showed significant interacting effect (p-value < 0.05) of MP-types and concentration during initial exposure phase (Week 1).

3.3 Impact of MPs on mussels microbiota

3.3.1 Bacterial community composition - taxonomic analyses

Taxonomic classification of the 16S rRNA amplicon sequences identified 32 phyla based on BLASTN search against the SILVA database. In the seawater sample, Rhodobacterales, Flavobacteriales, Actinomarinales, Microtrichales, and Planctomycetales were the top five most abundant orders. Microorganisms found on virgin MPs mostly belong to Rhodobacterales, Pseudomonadales,

Actinomycetales, Deltaproteobacteria - MBNT15, and Flavobacteriales, while those on weathered MPs mostly belong to Caulobacterales, Oceanospirillales, Parvibaculales, Rhodospirillales, and Planctomycetales. At the time mussels were acquired (before acclimation), the gut microbiota was abundant in Flavobacteriales, Fusobacteriales, Pirellulales, Rhodobacterales, and Microtrichales. After the acclimation process, the most abundant orders of mussel gut microbiota were Campylobacterales, Bacteroidales, Flavobacteriales, Vibrionales, and Alteromonadales.

Overall, throughout the MPs exposure and post-exposure depuration, mussel gut microbiota was dominated by phyla Proteobacteria and Bacteroidetes, followed by other significant phyla including Epsilonbacteraeota, Tenericutes, Chlamydiae, Actinobacteria, Fusobacteria, Planctomycetes, Firmicutes, and Verrucomicrobia (Fig. 4 and Supplementary Material 3). At the class level, the most abundant classes were Gammaproteobacteria, Bacteroidia, Alphaproteobacteria, Campylobacteria, Mollicutes, Chlamydiae, Fusobacteriia, Planctomycetacia, Deltaproteobacteria, and Clostridia. The most abundant orders were Flavobacteriales, Oceanospirillales, Vibrionales, Alteromonadales, Campylobacterales, Francisellales, Cardiobacteriales, Rhizobiales, Rhodobacterales, and Bacteroidales. Dynamics of mussel gut bacterial community compositions corresponding to experimental conditions and progression were displayed in Fig. 4 and Supplementary Material 3. Microbial diversity decreased significantly after the acclimation process. The abundance of order Flavobacteriales was higher in mussels that were exposed to weathered MPs during the period of exposure and 2 days after post-exposure depuration, but not after 8 days depuration. The abundance of Oceanospirillales was lower in MPs exposed mussels, especially in those exposed to "weathered" MPs in high concentration. Even after 8-day post-exposure depuration, the abundance of Oceanospirillales in mussels that were exposed to "weathered" MPs was still lower as compared with not exposed mussels. Similarly, the abundance of Chlamydiales was higher in mussels exposed to "weathered" MPs and high-concentration "virgin" MPs after 3-week and 6-week exposure, as well as after 2-day and 8-day post-exposure depuration.

As for samples of tank water that contains mussel excreta, microbiota was abundant in Flavobacteriales, Rhodobacterales, Rhizobiales, Campylobacterales, Thiotrichales, Oceanospirillales, Alteromonadales, Micrococcales, Pirellulales, and Milano-WF1B-44 (Gammaproteobacteria) (Fig. 5 and Supplementary Material 4).

3.3.2 Taxa that were affected by MPs exposure

For individual OTU at each time point, sequence read counts differences between the control and MPs exposed samples were examined using the non-parametric Wilcoxon test. Species/OTUs that have significantly higher or lower relative abundance p value < 0.05 were presented as heatmaps in Fig. 6 and Supplementary Material 5. According to the result of Wilcoxon test, totally 126 OTUs were identified that have significant difference in abundance in MPs exposed samples as compared with the control. In MPs exposed mussel gut samples, 57 OTUs have decreased abundance (Fig. 6a) and 69 OTUs have increased abundance (Fig. 6b) as compared with not exposed control mussel gut samples. Overall, the most abundant genera of mussel gut microbiota were Polaribacter, Neptuniibacter, Vibrio, Psychromonas, and Arcobacter. Therefore among these 126 OTUs, it is unsurprisingly to find 16 OTUs that belong to Polaribacter, 5 OTUs belong to Neptuniibacter, and 4 OTUs belong to Psychromonas. Notably, significantly changed Arcobacter (4 OTUs) were all in the list of increasing abundance (the “Up list”) and significantly changed Vibrio (1 OTU) was in the list of decreasing abundance (the “Down list”) for MPs exposed samples. Interestingly, 1 OTU of Bdellovibrio, which can infect and parasitize Vibrio, was found in the “Up list” for MPs exposed samples.

3.3.3 Metagenome functional prediction

The phylogenetic investigation of communities by reconstruction of unobserved states (PICRUSt) analysis was applied to predict functional profiling of microbial community. In this study, OTUs tables of the “Up” and “Down” lists were used for generating “virtual” metagenome of KEGG Ortholog abundances. Categorized by function, the dominant function was metabolism (83.5% of the “Up” list and 85.5% of the

328 “Down” list), followed by environmental information processing (8.2% of “Up, 9.9% of “Down”), cellular
329 processes (2.0% of “Up, 3.5% of “Down”), human diseases (3.7% of “Up, 0.6% of “Down”), and genetic
330 information processing (2.6% of “Up, 0.5% of “Down”)(Table 2). Specific to the “Up” list, pathways and
331 modules maybe of interest to this study include steroid biosynthesis, sesquiterpenoid and triterpenoid
332 biosynthesis, nitrogen metabolism, antimicrobial resistance, caprolactam degradation, and chloroalkane
333 and chloroalkene degradation. Specific to the “Down” list, pathways and modules of interest include
334 anoxygenic photosynthesis, secondary metabolite biosynthesis, sulfur metabolism, fluorobenzoate
335 degradation, chlorocyclohexane and chlorobenzene degradation, ethenylbenzene degradation, xylene
336 degradation, toluene degradation, dioxin degradation, and polycyclic aromatic hydrocarbon degradation.
337 Since the “Up” list consists of OTUs that have increased abundance in MPs-exposed mussel gut
338 microbiota and the “Down” list consists of OTUs that have decreased abundance, this may imply the
339 mussel gut microbiota had increased “Up” list-specific functions and decreased “Down” list- specific
340 functions after MPs exposure.

341 **3.3.4 Unique biomarkers**

342 The linear discriminant analysis effect size (LEfSe) analysis was applied to investigate taxonomic
343 differences and unique biomarkers from each condition. First, microbial communities of seawater
344 samples (input), unexposed (to MPs) mussel guts (mussels) and feces/tank water (output) were
345 compared. The analysis of LEfSe identified 17 and 16 differentially abundant microbial taxa from the
346 mussels and the output communities, and 70 differentially abundant microbial taxa from the seawater
347 community (Supplementary material 6). This result suggested that seawater microbiota is different from
348 mussel gut-related microbiota (mussels and output). Following, gut microbiota of MPs-exposed and
349 unexposed mussels were compared according to time progression of the experiment and results were
350 displayed in Fig. 7a-e (detailed list in Supplementary material 6). Most notably (and agree with above
351 mentioned result), taxa belonging to Chlamydiae were identified as differentially abundant in

"weathered" MPs exposed samples of 3 weeks, 6 weeks, 2-day depuration, and 8-day depuration. Other examples including: Rubritaleaceae was identified in "weathered" MPs exposed samples of 3 weeks, 6 weeks, and 2-day depuration; Verrucomicrobiales was identified in "weathered" MPs exposed samples of 6 weeks and 2-day depuration; Psychromonadaceae was identified in "virgin" MPs exposed samples of 6 weeks, 2-day depuration, and 8-day depuration; Xanthomonadales was identified in "virgin" MPs exposed samples of 1 week and 3 weeks; Flavobacteriales was identified in "virgin" MPs exposed samples of 1 week and 6 weeks. Results of LEfSe analysis revealed differentially abundant taxa in microbial communities, and these taxa could be potential unique biomarkers for representing their specific community for further studies. In addition, indicator species analysis was also performed and the overall outcome was similar to the result of LEfSe. A table presenting results from both analyses were presented in Supplementary Material 7.

4. DISCUSSION

MPs pollution in the environment all over the world has raised public concern [63]. Therefore, numerous environments were surveyed in order to evaluate the seriousness of MPs pollution, especially in the aquatic domain. For instance, a survey of an industrial harbor in Sweden found a very high concentration of MPs (102,000 particles m^{-3}, ~0.5 - 2mm) in seawater [87]. Furthermore, a recent article reported up to 1.9 million pieces m^{-2} of MPs (>63 μm) on the seafloor of Tyrrhenian Sea [88]. However, majority of environmental surveys were conducted using the manta trawl sampling with net mesh size 300 μm or larger [[89] and references therein]. A recent study has confirmed that sampling with a 100 μm mesh resulted in the collection of 2.5-fold greater MP concentration as compared with 333 μm mesh [90]. In other words, MPs with size smaller than 300 μm were overlooked by most of surveys and MPs concentrations reported in these surveys have underestimated MPs contamination in reality. In fact, a study surveying 770 personal care products for microbeads revealed that over 95% of particles in those

products were smaller than 300 µm in diameter [89]. Additionally, a survey at the Swedish coast found that up to 100,000 times higher concentrations of MPs was retained on an 80 µm mesh compared to a 450 µm mesh [91]. Similarly, a study surveying the South China Sea revealed not only concentrations of MPs were five orders of magnitude higher on a 44 µm mesh compared to a 300 µm mesh, but also smaller-size MPs (< 300 µm) contributed to 92 % of the total MPs count [92]. Hence, it is reasonable to expect even higher MPs concentrations if smaller mesh size filter (1 µm or nanometer range) were used in surveys. Based upon above reasoning and taking into account that current recognized environmental MPs concentration might be underestimated, the "High" MPs concentration was included in this experiment to better reflect such scenario.

In the seawater, aging and weathering processes are almost inevitable for MPs. These processes change physiochemical properties of MPs including surface area, oxygen groups, crystallinity, and sorption/leachate chemicals, and such changes can support further biofouling of MPs [93-95]. It has been shown that aging/weathering of MPs promotes their ingestion by marine animals such as zooplankton and Mediterranean mussels [52, 96]. In addition, microbial colonization could help low-density MPs to sink and increase MP residence time in the water column, and this would make MPs more available to marine animals [97, 98]. Therefore, besides two MPs concentrations, un-treated and seawater-treated MPs ("Virgin" and "Weathered" conditions) were also included in this study. According to 16S rRNA sequencing results, not only the microbiota of "Weathered" MPs had greater diversity (277 OTUs) than the microbiota of "Virgin" MPs (15 OTUs), but also community composition were different as only 3 OTUs were in common between the two microbiotas (Fig. 1a).

Gut microbiota alpha diversity and abundance of dominant taxa showed to be mainly influenced by exposure time and secondly by interaction of "time + MPs type" ("virgin" or "weathered") or "time + MPs concentration". The influence of time is more likely due to mussel aging, causing natural evolution of their microbiota, than by MPs exposure. Indeed, further statistical analysis confirmed that assumption

400 with no significant change observed for diversity indices when time was grouped as independent
401 variable. This result was not surprising since diversity indices only described drastic change in microbial
402 community structure but fail to detect fine changes – that happened when subtle alteration of mussel
403 culture was triggered by MPs treatment. Consistently with these results, significant change was observed
404 by considering change of microbial community structure at the most detail OTUs level. Indeed,
405 hierarchical cluster analysis cluster and non-metric multidimensional scaling together with PERMANOVA
406 analysis, confirmed the influence of exposure time on microbial community structure, but also revealed
407 a significant effect of the type of MPs, as well as interaction of variables (type of MPs with time and with
408 concentration). These analyses demonstrated that MPs significantly influenced composition of mussel
409 gut microbiota of several OTUs.
410 During the 6-week MPs exposure, more gut microbiota OTUs had their abundance affected by
411 “Weathered” MPs than by “Virgin” MPs overall (Table 3). Similarly, more OTUs had their abundance
412 affected by “High” concentration of MPs than by “Low” concentration of MPs (Table 3). It is not
413 surprising that “High” concentration MPs prompted greater impacts on mussel gut microbiota than
414 “Low” concentration MPs. Interestingly, “Weathered” MPs, even in “Low” concentration, could generate
415 comparable or sometimes greater alteration in gut microbiota than “Virgin” “High” concentration of MPs
416 (Table 3). Our results of (a) “Weathered” MPs carried greater microbial diversity and (b) “Weathered”
417 MPs prompted stronger alteration to gut microbiota of mussels remind us not to underestimate
418 potential impacts from MP-associated microorganisms. Indeed, due to the small size of MPs, the
419 amounts of chemicals that can be released or adsorbed are limited. By contrast, even very few numbers
420 of microorganisms carried by MPs could multiply into significant populations in a short period of time as
421 long as conditions allow. Such circumstance surely will affect microbiota of the host, especially if
422 pathogen was involved. As a matter of fact, from the statistical point of view, difference in a small
423 amount of OTUs is not enough to alter alpha diversity indices and proclaim changes in community

424 composition. However, from food safety and public health point of views, even a single OTU difference,
425 if it involved a pathogenic species, could have serious consequence. For example, certain toxigenic
426 *Shigella spp.* has the infectious dose as low as less than 10 organisms [99]. Therefore, for above reasons
427 and as recommended by previous literature [27], it is absolutely necessary to further study relationship
428 between MPs and microbiota.
429 As mentioned in the introduction, only a handful of studies have investigated effects of MPs on gut
430 microbiota with model animal zebrafish and mice, and alteration in microbiota were reported [34, 57-
431 59]. In the gut of adult zebrafish, high throughput sequencing revealed significant changes of 29 OTUs
432 after 14-day exposure to 1 mg/L of polystyrene [57]. Similar study conducted on mice revealed
433 significant changes of 310 and 160 OTUs after 5-week exposure to 1 mg/L of polystyrene in 0.5 and
434 50 µm respectively [59]. Both studies have concluded the risk of MPs exposure affecting animal health.
435 However, to our knowledge, no existing study has investigated impacts of MP-exposure on mussel gut
436 microbiota, nor effect of "virgin" and "weathered" MPs on microbiota of any animal. It is also worth
437 mentioning that the majority of MP-exposure experiments were conducted with polystyrene, while
438 polyethylene is prevailing in the water bodies of the environment [100].
439 Impacts on mussel gut microbiota after MPs exposure were revealed in this study. According to the
440 result of Wilcoxon test, within the “Up list”, potential human pathogens were found (16 OTUs) including
441 Arcobacter, Candidatus Berkiella, Candidatus Megaira, Cardiobacteriaceae, Chlamydiales, Candidatus
442 Rhabdochlamydia, Criblamydiaceae, Clostridiales, Legionellaceae, *Mycoplasma*, *Psychrobacter*, and
443 *Shewanella* (KEGG Pathogen Resource, https://www.genome.jp/kegg/genome/pathogen.html). Potential
444 fish, mollusca, or marine eukaryotes pathogens were found as well (11 OTUs) including Aquimarina,
445 Candidatus Jidaibacter, Francisella, Moritella, Rickettsiella, and Tenacibaculum (https://www.eurl-fish-
446 crustacean.eu/). Eleven OTUs including Colwellia, Oleispira, Polaribacter, and Sphingorhabdus may
447 involve in biopolymer degradation (http://www.cazy.org/); 9 OTUs including Arcobacter, Colwellia,

448 Loktanella, and Owenweeksia may involve in biofilm formation [101-104]. Four OTUs of Blastopirellula
449 may involve in nitrification [105]. In the "Down list", potential human pathogens were found (5 OTUs)
450 including *Legionella*, *Mycoplasma*, *Shewanella*, and *Vibrio* (KEGG Pathogen Resource,
451 https://www.genome.jp/kegg/genome/pathogen.html). Potential fish, mollusca, or marine eukaryotes
452 pathogens were found as well (4 OTUs) including Aquimarina, Roseovarius, and Tenacibaculum
453 (https://www.eurl-fish-crustacean.eu/). Thirteen OTUs including Cyclobacteriaceae, Polaribacter,
454 Psychrilyobacter, Saccharospirillaceae, and Zobellia may involve in biopolymer degradation
455 (http://www.cazy.org/, [106, 107]) ; 1 OTU of Candidatus Sericytochromatia may involve in biofilm
456 formation [108]. Four OTUs including Ahrensia, Pirellula, and Sulfitobacter may involve in sulfur cycling
457 [109-111].
458 The result of PICRUSt analysis further suggested functions that might be impacted by MPs exposure in
459 mussel gut microbiota. Within the potentially increased functions, the steroid biosynthesis pathway and
460 the sesquiterpenoid/triterpenoid biosynthesis pathway are connected because steroids can be produced
461 from terpenoid precursors [112]. Other potentially increased functions include nitrogen metabolism,
462 antimicrobial resistance, caprolactam degradation, and chloroalkane and chloroalkene degradation.
463 Intriguingly, caprolactam is the precursor to Nylon 6 [113]; certain chloroalkane (e.g. chloromethane) are
464 used for the production of organosilicon compounds such as sealants, while chloroethene (a type of
465 chloroalkene), also known as vinyl chloride, is used to produce the polymer polyvinyl chloride (PVC)
466 [114]. Potentially decreased functions include anoxygenic photosynthesis, secondary metabolite
467 biosynthesis, sulfur metabolism, dioxin degradation, polycyclic aromatic hydrocarbon degradation,
468 fluorobenzoate degradation, chlorocyclohexane and chlorobenzene degradation, ethenylbenzene
469 degradation, xylene (dimethylbenzene) degradation, and toluene (methylbenzene) degradation.
470 Therefore, degradation of benzene ring-containing molecules might be affected presumably. In a
471 previous study in mice [58], influence on predicted metabolic pathways of microbial gut community

were also observed after MP-exposure. Mice that exposed to 1 mg/L polystyrene MPs for 6-weeks had significant changes in main metabolic pathways of the gut microbial community, including pyruvate metabolism, tyrosine metabolism, fatty acid biosynthesis, and bacterial invasion of epithelial cell. For future studies, metatranscriptomic analysis may be applied to confirm metabolic pathways changes in mussels gut microbial community due to MP-exposure.

The depuration process for seafood was originally designed to allow purging of physical impurities (such as sand and silt) and biological contaminants (such as *Salmonella enterica* subsp. *enterica*, serovar Typhi and *Escherichia coli*). Depuration of bivalves (usually for 48 hours) before retail sale is mandatory in many countries [72]. Based upon this concept, a post-exposure depuration was included in this study to further monitor mussel gut microbiota after MPs were eliminated from tanks. Even after 8-day post-exposure depuration, gut microbiota of mussels that were exposed to “High” concentration MPs still have more OTUs with altered abundance as compared with gut microbiota of “Low” concentration MPs-exposed mussels (24 vs. 16 OTUs). By contrast, after 8-day depuration, gut microbiota of mussels that were exposed to “Virgin” MPs and "Weathered" MPs have similar numbers of OTUs with altered abundance (19 and 21 OTUs, separately). Such result suggests that MPs-affected gut microbiota might not be able to recover in a short period of time after eliminating the pollutant, neither the possibility of long-term modification on microbiota could be excluded.

In this study, water samples from each tank were also collected at every time point. Hierarchical cluster analysis showed that microbiota of samples from non-exposed tanks (control) are always in different clusters than samples from "virgin-high", "weathered-low", and "weathered-high" MP-exposed tanks even after post-exposure depuration (Fig. 2). These results suggest that MP-ingestion by mussels could also influence microbiota of the surrounding environment. Indeed, after ingestion, MPs can be incorporated into faecal pellets. Such MPs-containing faecal pellets carrying MP-affected gut microbiota releasing back to the water column could contribute to affection in microbiota of surrounding seawater

and present result supports this hypothesis. Furthermore, previous study has suggested that MP-associated faecal pellets could have decreased sinking rate and consequently may potentially lower the efficiency of the biological pump [115]. Taken together, MPs pollution can not only affect animal health through gut microbiota, but also further influence the environmental ecosystem including microbiota, biodiversity, and even biogeochemical cycles.

5. CONCLUSIONS

Undeniably, MPs are now widespread in the ecosystem and present in the life of many living organisms. In this study, we focused on investigating impacts of MP-exposure on mussel gut microbiota. As compared with non-exposed mussels, alteration of gut microbiota was observed after mussels were exposed to MPs for 1 week, 3 weeks, 6 weeks, even after 8-day post-exposure depuration. Such alteration of gut microbiota was greater in mussels exposed to high concentration MPs than low concentration MPs; greater in mussels exposed to "weathered" MPs than "virgin" MPs. Through faecal pellets, microbiota of tank water was as well altered, suggesting potential consequent influence on microbiota of the surrounding environment. Potential human pathogens were found among OTUs with increased abundance induced by MP-exposure, and some of them retained higher abundance even after 8 days depuration. In conclusion, the present results have shown that MP-exposure can alter mussel gut microbiota. As a consequence, further research might consider alteration in gut microbiota could potentially: (1) affect the animal health therefore affect food quality; (2) promote certain pathogens therefore affect food safety; (3) may affect the environmental microbiota therefore influence the biodiversity of the ecosystem.

6. Funding

This work has been financially supported by the European Union European Regional Development Fund (ERDF), the French State, the French Region Hauts-de-France and Ifremer, in the framework of the

project CPER MARCO 2015-2020, and sequencing cost were partially supported by the Structure Fédérative de Recherche (SFR) Campus de la mer.

7. Acknowledgments

The authors would like to thank Tristan Biard and Stéphanie Bougeard for their help with R script, Capucine Bialais and Nicolas Rayappa for microalgae culture, and Jeremy Denis for acquiring mussels.

8. Conflicts of Interest

The authors declare no conflict of interest.

9. Figure Legends

Figure 1. 16S rRNA gene sequences analysis. Operational taxonomic units (OTUs) shared among different sample groups. (a) OTUs shared among input microbiota (filtered seawater, virgin MPs, and weathered MPs), mussel gut microbiota, and output microbiota (feces/tank water). (b) OTUs shared among "virgin" MPs microbiota, "weathered" MPs microbiota, and mussel gut microbiota.

Figure 2. Hierarchical clustering of control and tank water/feces microbial diversity based on Bray–Curtis dissimilarities calculated on double square root transformed number of OTUs reads. "*" in the dendrogram indicate similarities between bifurcations/samples, based on the SIMPROF significance test. The dash line indicate arbitrary cluster separation, while solid lines on the bottom represent cluster separation according the sample origin. Abbreviations: 1W – 1-week; 3W – 3 weeks; 6W – 6 weeks; D2d – depuration 2-day; D8d – depuration 8-day; C – control; VL – virgin low; VH – virgin high; WL – weathered low; WH – weathered high.

Figure 3. Non-metric multidimensional scaling (NMDS) on the gut microbiota community. The analysis was performed on the gut bacterial OTUs composition during the 6-week MPs exposure (1, 3 and 6 weeks) and depuration (2 and 8 days). Shapes of symbols correspond to different treatments and colors of symbols correspond to different time points. Abbreviations: C – control; VL – virgin low; VH – virgin high; WL – weathered low; WH – weathered high; "C": control without MPs; "VL": virgin MPs at low concentration; "VH": virgin MPs at high concentration; "WL": weathered MPs at low concentration; "WH": weathered MPs at high concentration; Depu2 – depuration 2-day; Depu8 – depuration 8-day.

Figure 4. Microbial community composition of mussel gut microbiota (at order level). Taxa were grouped first by phylum then by class. Bacteroidetes was presented in shades of green; Chlamydiae was presented in yellow; α, δ, and β Proteobacteria were presented in shades of blue; γ Proteobacteria were presented in shades of purple. Taxa ratios in the community were detailed in Supplementary material 3. Abbreviations: Accli.S – acclimation start; Accli.F – acclimation finish; 1W – 1 week; 3W – 3 weeks; 6W – 6 weeks; D2d – depuration 2-day; D8d – depuration 8-day; C – control; VL – virgin low; VH – virgin high; WL – weathered low; WH – weathered high.

Figure 5. Microbial community composition of mussel feces and tank water (at order level). Taxa were grouped first by phylum then by class. Actinobacteria was presented in shades of orange; Bacteroidetes was presented in shades of green; Chlamydiae was presented in yellow; α, δ, and β Proteobacteria were presented in shades of blue; γ Proteobacteria were presented in shades of purple. Taxon ratios in the community were detailed in Supplementary material 4. Abbreviations: 1W – 1 week; 3W – 3 weeks; 6W – 6 weeks; D8d – depuration 8-day; C – control; VL – virgin low; VH – virgin high; WL – weathered low; WH – weathered high.

Figure 6. OTUs that have significant difference in abundance in MPs exposed samples as compared with the control. (a) OTUs (as shown in their taxa) with decreased abundance. (b) OTUs with increased abundance. Identification of OTUs (including accession number) and information of significant changes were detailed in Supplementary material 5. Abbreviations: 1W – 1-week; 3W – 3 weeks; 6W – 6 weeks; D2d – depuration 2-day; D8d – depuration 8-day; C – control; VL – virgin low; VH – virgin high; WL – weathered low; WH – weathered high.

Figure 7. Linear discriminant analysis effect size (LEfSe) for identifying potential unique biomarkers in each sample group. (a) Sample groups: input microbiota, mussel gut microbiota, and output microbiota. (b) Mussel gut microbiota after 1 week exposure, (c) Mussel gut microbiota after 3 weeks exposure, (d) Mussel gut microbiota after 6 weeks exposure, (e) Mussel gut microbiota after 2 days depuration, (f) Mussel gut microbiota after 8 days depuration. Details were listed in Supplementary material 7.

10. Table Legends

Table 1. PERMANOVA (Adonis) results for gut microbiota (OTUs) communities structures during the 6-week MPs exposure, based on Bray-Curtis distance.

Table 2. Metagenome functional prediction for the "Up" and "Down" taxa. The "phylogenetic investigation of communities by reconstruction of unobserved states (PICRUSt)" analysis was performed and functions were categorized according to the KEGG Orthology database.

589 **Table 3.** Numbers of operational taxonomical unit (OTU) that have changed in abundance (increase or
590 decrease) by exposing to MPs (condition “virgin” or “weathered”, concentration “low” or “high”) as
591 compared with the control.
592

593 ## 11. Supplementary Material Legends

594

595 **Supplementary material 1.** Indices for alpha diversity and abundance of dominant taxa. The box plot
596 shows mean values and standard deviation of the richness (Chao), Equitability (Simpson and Shannon)
597 and dominance (Berger-Parker) estimators for gut microbiota community during the 6 weeks MPs
598 exposition (1, 3 and 6 weeks) and depuration (2 and 8 days). Each box correspond to a treatment with
599 “C”: control without MPs, “VL”: virgin MPs at low concentration, “VH”: virgin MPs at high concentration,
600 “WL”: weathered MPs at low concentration and “WH”: weathered MPs at high concentration.
601

602 **Supplementary material 2.** Hierarchical clustering of microbial diversity for controls and mussels
603 exposed to microplastics was calculated on the 1370 most abundant OTUs representing 99% of all reads.
604 The dendrogram, based on Bray–Curtis dissimilarities, was constructed after double square root
605 transformed of OTUs reads number. Similarities between bifurcations/samples, based on the SIMPROF
606 significance test, were indicated by red dash lines.
607

608 **Supplementary material 3.** Microbial community composition of mussel gut microbiota (at order level).
609 Taxa were grouped first by phylum then by class. Bacteroidetes was presented in shades of green;
610 Chlamydiae was presented in yellow; α, δ, and β Proteobacteria were presented in shades of blue; γ
611 Proteobacteria were presented in shades of purple. Taxon ratios in the community were detailed in
612 Supplementary material 3. Abbreviations: Accli.S – acclimation start; Accli.F – acclimation finish; 1W – 1

613 week; 3W – 3 weeks; 6W – 6 weeks; D2d – depuration 2-day; D8d – depuration 8-day; C – control; VL –
614 virgin low; VH – virgin high; WL – weathered low; WH – weathered high.
615
616 **Supplementary material 4.** Microbial community composition of mussel feces and tank water (at order
617 level). Taxa were grouped first by phylum then by class. Actinobacteria was presented in shades of
618 orange; Bacteroidetes was presented in shades of green; Chlamydiae was presented in yellow; α, δ, and
619 β Proteobacteria were presented in shades of blue; γ Proteobacteria were presented in shades of purple.
620 Taxon ratios in the community were detailed in Supplementary material 4. Abbreviations: 1W – 1 week;
621 3W – 3 weeks; 6W – 6 weeks; D8d – depuration 8-day; C – control; VL – virgin low; VH – virgin high; WL –
622 weathered low; WH – weathered high.
623
624 **Supplementary material 5.** OTUs that have significant difference in abundance in MPs exposed samples
625 as compared with the control. (a) OTUs (as shown in their taxa) with decreased abundance. (b) OTUs
626 with increased abundance. Identification of OTUs (including accession number) and information of
627 significant changes were detailed in Supplementary material 5. Abbreviations: 1W – 1-week; 3W – 3
628 weeks; 6W – 6 weeks; D2d – depuration 2-day; D8d – depuration 8-day; C – control; VL – virgin low; VH –
629 virgin high; WL – weathered low; WH – weathered high.

630 **Supplementary material 6.** Linear discriminant analysis effect size (LEfSe) for identifying potential unique
631 biomarkers in each sample group. (a) Sample groups: input microbiota, mussel gut microbiota, and
632 output microbiota. (b) Mussel gut microbiota after 1 week exposure, (c) Mussel gut microbiota after 3
633 weeks exposure, (d) Mussel gut microbiota after 6 weeks exposure, (e) Mussel gut microbiota after 2
634 days depuration, (f) Mussel gut microbiota after 8 days depuration. Details were listed in Supplementary
635 material 7.
636

Supplementary material 7. Taxa that contributed mostly to assemblage dissimilarities between different groups – compare results from indicator species analysis and linear discriminant analysis effect size (LEfSe) program. "*/*" represent taxonomic groups identified both with "indicator analysis" and "Lefse analysis", "*/-" corresponded to taxonomic groups only identified with "indicator analysis" and "-/*" represent taxonomic groups only identified with "Lefse analysis". Significance *p*-value codes for "Indicator analysis" were 0: '***', 0.001 : '**', 0.01 : '*'. Abbreviations: 1W – 1-week; 3W – 3 weeks; 6W – 6 weeks; D2d – depuration 2-day; D8d – depuration 8-day; C – control; VL – virgin low; VH – virgin high; WL – weathered low; WH – weathered high.Legends: control "C", virgin MP low concentration "VL", virgin MP high concentration "VH", weathered MP low concentration "WL" and weathered MP high concentration "WH".

12. REFERENCES

1. Ryan, P.G. and C.L. Moloney, *Marine litter keeps increasing.* Nature, 1993. **361**(6407): p. 23-23.
2. Worm, B., H.K. Lotze, I. Jubinville, C. Wilcox, and J. Jambeck, *Plastic as a Persistent Marine Pollutant.* Annual Review of Environment and Resources, 2017. **42**(1): p. 1-26.
3. Geyer, R., J.R. Jambeck, and K.L. Law, *Production, use, and fate of all plastics ever made.* Sci Adv, 2017. **3**(7): p. e1700782.
4. Jambeck, J.R., R. Geyer, C. Wilcox, T.R. Siegler, M. Perryman, A. Andrady, R. Narayan, and K.L. Law, *Marine pollution. Plastic waste inputs from land into the ocean.* Science, 2015. **347**(6223): p. 768-71.
5. *Ghosts beneath the waves: Ghost gear's catastrophic impact on our oceans, and the urgent action needed from industry*. 2018, London, UK: World Society for the Protection of Animals.
6. Peng, L., D. Fu, H. Qi, C.Q. Lan, H. Yu, and C. Ge, *Micro- and nano-plastics in marine environment: Source, distribution and threats — A review.* Science of The Total Environment, 2020. **698**: p. 134254.
7. Karbalaei, S., P. Hanachi, T.R. Walker, and M. Cole, *Occurrence, sources, human health impacts and mitigation of microplastic pollution.* Environmental Science and Pollution Research, 2018. **25**(36): p. 36046-36063.
8. Lavers, J.L., L. Dicks, M.R. Dicks, and A. Finger, *Significant plastic accumulation on the Cocos (Keeling) Islands, Australia.* Scientific Reports, 2019. **9**(1): p. 7102.
9. Obbard, R.W., S. Sadri, Y.Q. Wong, A.A. Khitun, I. Baker, and R.C. Thompson, *Global warming releases microplastic legacy frozen in Arctic Sea ice.* Earth's Future, 2014. **2**(6): p. 315-320.
10. Peeken, I., S. Primpke, B. Beyer, J. Gütermann, C. Katlein, T. Krumpen, M. Bergmann, L. Hehemann, et al., *Arctic sea ice is an important temporal sink and means of transport for microplastic.* Nature Communications, 2018. **9**(1): p. 1505.

11. Woodall, L.C., A. Sanchez-Vidal, M. Canals, G.L. Paterson, R. Coppock, V. Sleight, A. Calafat, A.D. Rogers, et al., *The deep sea is a major sink for microplastic debris.* R Soc Open Sci, 2014. **1**(4): p. 140317.
12. Choy, C.A., B.H. Robison, T.O. Gagne, B. Erwin, E. Firl, R.U. Halden, J.A. Hamilton, K. Katija, et al., *The vertical distribution and biological transport of marine microplastics across the epipelagic and mesopelagic water column.* Scientific Reports, 2019. **9**(1): p. 7843.
13. Brandon, J., M. Goldstein, and M.D. Ohman, *Long-term aging and degradation of microplastic particles: Comparing in situ oceanic and experimental weathering patterns.* Mar Pollut Bull, 2016. **110**(1): p. 299-308.
14. Amaral-Zettler, L.A., E.R. Zettler, and T.J. Mincer, *Ecology of the plastisphere.* Nature Reviews Microbiology, 2020. **18**(3): p. 139-151.
15. Cole, M., P. Lindeque, E. Fileman, C. Halsband, R. Goodhead, J. Moger, and T.S. Galloway, *Microplastic ingestion by zooplankton.* Environ Sci Technol, 2013. **47**(12): p. 6646-55.
16. Van Cauwenberghe, L., M. Claessens, M.B. Vandegehuchte, and C.R. Janssen, *Microplastics are taken up by mussels (Mytilus edulis) and lugworms (Arenicola marina) living in natural habitats.* Environmental Pollution, 2015. **199**: p. 10-7.
17. Rochman, C.M., A. Tahir, S.L. Williams, D.V. Baxa, R. Lam, J.T. Miller, F.-C. Teh, S. Werorilangi, et al., *Anthropogenic debris in seafood: Plastic debris and fibers from textiles in fish and bivalves sold for human consumption.* Scientific Reports, 2015. **5**: p. 14340.
18. Van Cauwenberghe, L. and C.R. Janssen, *Microplastics in bivalves cultured for human consumption.* Environ Pollut, 2014. **193**: p. 65-70.
19. Nelms, S.E., J. Barnett, A. Brownlow, N.J. Davison, R. Deaville, T.S. Galloway, P.K. Lindeque, D. Santillo, et al., *Microplastics in marine mammals stranded around the British coast: ubiquitous but transitory?* Scientific Reports, 2019. **9**(1): p. 1075.
20. Lusher, A.L., G. Hernandez-Milian, J. O'Brien, S. Berrow, I. O'Connor, and R. Officer, *Microplastic and macroplastic ingestion by a deep diving, oceanic cetacean: the True's beaked whale Mesoplodon mirus.* Environ Pollut, 2015. **199**: p. 185-91.
21. Cole, M., P. Lindeque, E. Fileman, C. Halsband, and T.S. Galloway, *The impact of polystyrene microplastics on feeding, function and fecundity in the marine copepod Calanus helgolandicus.* Environ Sci Technol, 2015. **49**(2): p. 1130-7.
22. Browne, M.A., A. Dissanayake, T.S. Galloway, D.M. Lowe, and R.C. Thompson, *Ingested microscopic plastic translocates to the circulatory system of the mussel, Mytilus edulis (L).* Environ Sci Technol, 2008. **42**(13): p. 5026-31.
23. Collard, F., B. Gilbert, P. Compère, G. Eppe, K. Das, T. Jauniaux, and E. Parmentier, *Microplastics in livers of European anchovies (Engraulis encrasicolus, L.).* Environmental Pollution, 2017. **229**: p. 1000-1005.
24. Kolandhasamy, P., L. Su, J. Li, X. Qu, K. Jabeen, and H. Shi, *Adherence of microplastics to soft tissue of mussels: A novel way to uptake microplastics beyond ingestion.* Sci Total Environ, 2018. **610-611**: p. 635-640.
25. Wright, S.L., R.C. Thompson, and T.S. Galloway, *The physical impacts of microplastics on marine organisms: a review.* Environ Pollut, 2013. **178**: p. 483-92.
26. Lithner, D., Å. Larsson, and G. Dave, *Environmental and health hazard ranking and assessment of plastic polymers based on chemical composition.* Science of The Total Environment, 2011. **409**(18): p. 3309-3324.
27. Fackelmann, G. and S. Sommer, *Microplastics and the gut microbiome: How chronically exposed species may suffer from gut dysbiosis.* Marine Pollution Bulletin, 2019. **143**: p. 193-203.

28. Sussarellu, R., M. Suquet, Y. Thomas, C. Lambert, C. Fabioux, M.E.J. Pernet, N. Le Goïc, V. Quillien, et al., *Oyster reproduction is affected by exposure to polystyrene microplastics.* Proceedings of the National Academy of Sciences, 2016. **113**(9): p. 2430-2435.
29. Murphy, F. and B. Quinn, *The effects of microplastic on freshwater Hydra attenuata feeding, morphology & reproduction.* Environ Pollut, 2018. **234**: p. 487-494.
30. Lo, H.K.A. and K.Y.K. Chan, *Negative effects of microplastic exposure on growth and development of Crepidula onyx.* Environ Pollut, 2018. **233**: p. 588-595.
31. Capolupo, M., S. Franzellitti, P. Valbonesi, C.S. Lanzas, and E. Fabbri, *Uptake and transcriptional effects of polystyrene microplastics in larval stages of the Mediterranean mussel Mytilus galloprovincialis.* Environmental Pollution, 2018. **241**: p. 1038-1047.
32. Blarer, P. and P. Burkhardt-Holm, *Microplastics affect assimilation efficiency in the freshwater amphipod Gammarus fossarum.* Environ Sci Pollut Res Int, 2016. **23**(23): p. 23522-23532.
33. Ju, H., D. Zhu, and M. Qiao, *Effects of polyethylene microplastics on the gut microbial community, reproduction and avoidance behaviors of the soil springtail, Folsomia candida.* Environmental Pollution, 2019. **247**: p. 890-897.
34. Qiao, R., C. Sheng, Y. Lu, Y. Zhang, H. Ren, and B. Lemos, *Microplastics induce intestinal inflammation, oxidative stress, and disorders of metabolome and microbiome in zebrafish.* Science of The Total Environment, 2019. **662**: p. 246-253.
35. O'Donovan, S., N.C. Mestre, S. Abel, T.G. Fonseca, C.C. Carteny, B. Cormier, S.H. Keiter, and M.J. Bebianno, *Ecotoxicological Effects of Chemical Contaminants Adsorbed to Microplastics in the Clam Scrobicularia plana.* Frontiers in Marine Science, 2018. **5**: p. 143.
36. Sommer, F., J.M. Anderson, R. Bharti, J. Raes, and P. Rosenstiel, *The resilience of the intestinal microbiota influences health and disease.* Nature Reviews Microbiology, 2017. **15**(10): p. 630-638.
37. O'Brien, P.A., N.S. Webster, D.J. Miller, and D.G. Bourne, *Host-Microbe Coevolution: Applying Evidence from Model Systems to Complex Marine Invertebrate Holobionts.* mBio, 2019. **10**(1): p. e02241-18.
38. Man, W.H., W.A.A. de Steenhuijsen Piters, and D. Bogaert, *The microbiota of the respiratory tract: gatekeeper to respiratory health.* Nature Reviews Microbiology, 2017. **15**(5): p. 259-270.
39. Kau, A.L., P.P. Ahern, N.W. Griffin, A.L. Goodman, and J.I. Gordon, *Human nutrition, the gut microbiome and the immune system.* Nature, 2011. **474**(7351): p. 327-336.
40. Turnbaugh, P.J., R.E. Ley, M. Hamady, C.M. Fraser-Liggett, R. Knight, and J.I. Gordon, *The Human Microbiome Project.* Nature, 2007. **449**(7164): p. 804-810.
41. Walker, W.A., *Chapter 25 - Dysbiosis*, in *The Microbiota in Gastrointestinal Pathophysiology - Implications for Human Health, Prebiotics, Probiotics, and Dysbiosis*, M.H. Floch, Y. Ringel, and W. Allan Walker, Editors. 2017, Academic Press: Boston. p. 227-232.
42. von Moos, N., P. Burkhardt-Holm, and A. Köhler, *Uptake and Effects of Microplastics on Cells and Tissue of the Blue Mussel Mytilus edulis L. after an Experimental Exposure.* Environmental Science & Technology, 2012. **46**(20): p. 11327-11335.
43. Wegner, A., E. Besseling, E.M. Foekema, P. Kamermans, and A.A. Koelmans, *Effects of nanopolystyrene on the feeding behavior of the blue mussel (Mytilus edulis L.).* Environmental Toxicology and Chemistry, 2012. **31**(11): p. 2490-7.
44. Fernández, B. and M. Albentosa, *Dynamic of small polyethylene microplastics (≤10 μm) in mussel's tissues.* Marine Pollution Bulletin, 2019. **146**: p. 493-501.
45. Rist, S., I.M. Steensgaard, O. Guven, T.G. Nielsen, L.H. Jensen, L.F. Møller, and N.B. Hartmann, *The fate of microplastics during uptake and depuration phases in a blue mussel exposure system.* Environmental Toxicology and Chemistry, 2019. **38**(1): p. 99-105.

765 46. Qu, X., L. Su, H. Li, M. Liang, and H. Shi, *Assessing the relationship between the abundance and*
766 *properties of microplastics in water and in mussels.* Sci Total Environ, 2018. **621**: p. 679-686.
767 47. Catarino, A.I., V. Macchia, W.G. Sanderson, R.C. Thompson, and T.B. Henry, *Low levels of*
768 *microplastics (MP) in wild mussels indicate that MP ingestion by humans is minimal compared to*
769 *exposure via household fibres fallout during a meal.* Environmental Pollution, 2018. **237**: p. 675-
770 684.
771 48. Kesy, K., A. Hentzsch, F. Klaeger, S. Oberbeckmann, S. Mothes, and M. Labrenz, *Fate and stability*
772 *of polyamide-associated bacterial assemblages after their passage through the digestive tract of*
773 *the blue mussel Mytilus edulis.* Marine Pollution Bulletin, 2017. **125**(1-2): p. 132-138.
774 49. Santana, M.F.M., F.T. Moreira, C.D.S. Pereira, D.M.S. Abessa, and A. Turra, *Continuous Exposure*
775 *to Microplastics Does Not Cause Physiological Effects in the Cultivated Mussel Perna perna.*
776 Archives of Environmental Contamination and Toxicology, 2018. **74**: p. 594-604.
777 50. Gandara, E.S., Pablo Pena, C.R. Nobre, P. Resaffe, C.D.S. Pereira, and F. Gusmão, *Leachate from*
778 *microplastics impairs larval development in brown mussels.* Water Research, 2016. **106**: p. 364-
779 370.
780 51. Paul-Pont, I., C. Lacroix, C. González Fernández, H. Hégaret, C. Lambert, N. Le Goïc, L. Frère, A.-L.
781 Cassone, et al., *Exposure of marine mussels Mytilus spp. to polystyrene microplastics: Toxicity*
782 *and influence on fluoranthene bioaccumulation.* Environmental Pollution, 2016. **216**: p. 724-737.
783 52. Bråte, I.L.N., M. Blázquez, S.J. Brooks, and K.V. Thomas, *Weathering impacts the uptake of*
784 *polyethylene microparticles from toothpaste in Mediterranean mussels (M. galloprovincialis).*
785 Science of The Total Environment, 2018. **626**: p. 1310-1318.
786 53. Brandts, I., M. Teles, A.P. Gonçalves, A. Barreto, L. Franco-Martinez, A. Tvarijonaviciute, M.A.
787 Martins, A.M.V.M. Soares, et al., *Effects of nanoplastics on Mytilus galloprovincialis after*
788 *individual and combined exposure with carbamazepine.* Science of The Total Environment, 2018.
789 **643**: p. 775-784.
790 54. Li, Q., C. Sun, Y. Wang, H. Cai, L. Li, J. Li, and H. Shi, *Fusion of microplastics into the mussel byssus.*
791 Environmental Pollution, 2019. **252**: p. 420-426.
792 55. Avio, C.G., S. Gorbi, M. Milan, M. Benedetti, D. Fattorini, G. d'Errico, M. Pauletto, L. Bargelloni, et
793 al., *Pollutants bioavailability and toxicological risk from microplastics to marine mussels.*
794 Environmental Pollution, 2015. **198**: p. 211-222.
795 56. Détrée, C. and C. Gallardo-Escárate, *Polyethylene microbeads induce transcriptional responses*
796 *with tissue-dependent patterns in the mussel Mytilus galloprovincialis.* Journal of Molluscan
797 Studies, 2017. **83**(2): p. 220-225.
798 57. Jin, Y., J. Xia, Z. Pan, J. Yang, W. Wang, and Z. Fu, *Polystyrene microplastics induce microbiota*
799 *dysbiosis and inflammation in the gut of adult zebrafish.* Environmental Pollution, 2018. **235**: p.
800 322-329.
801 58. Jin, Y., L. Lu, W. Tu, T. Luo, and Z. Fu, *Impacts of polystyrene microplastic on the gut barrier,*
802 *microbiota and metabolism of mice.* Science of The Total Environment, 2019. **649**: p. 308-317.
803 59. Lu, L., Z. Wan, T. Luo, Z. Fu, and Y. Jin, *Polystyrene microplastics induce gut microbiota dysbiosis*
804 *and hepatic lipid metabolism disorder in mice.* Science of The Total Environment, 2018. **631-632**:
805 p. 449-458.
806 60. Wan, Z., C. Wang, J. Zhou, M. Shen, X. Wang, Z. Fu, and Y. Jin, *Effects of polystyrene microplastics*
807 *on the composition of the microbiome and metabolism in larval zebrafish.* Chemosphere, 2019.
808 **217**: p. 646-658.
809 61. Caruso, G., C. Pedà, S. Cappello, M. Leonardi, R. La Ferla, A. Lo Giudice, G. Maricchiolo, C. Rizzo,
810 et al., *Effects of microplastics on trophic parameters, abundance and metabolic activities of*
811 *seawater and fish gut bacteria in mesocosm conditions.* Environmental Science and Pollution
812 Research, 2018. **25**(30): p. 30067-30083.

62. Zhu, B.-K., Y.-M. Fang, D. Zhu, P. Christie, X. Ke, and Y.-G. Zhu, *Exposure to nanoplastics disturbs the gut microbiome in the soil oligochaete Enchytraeus crypticus.* Environmental Pollution, 2018. **239**: p. 408-415.
63. Dalberg Advisors, W. de Wit, and N. Bigaud, *No Plastic in Nature: assessing plastic ingestion from nature to people*. 2019: Gland, Switzerland.
64. Fenske, C., *The Ecological Importance of Mussels, Their Effect on Water Quality and Their Possible Use for Coastal Zone Management*, in *Baltic Coastal Ecosystems. Central and Eastern European Development Studies*, G. Schernewski and U. Schiewer, Editors. 2002, Springer: Berlin, Heidelberg.
65. Azizi, G., M. Akodad, M. Baghour, M. Layachi, and A. Moumen, *The use of Mytilus spp. mussels as bioindicators of heavy metal pollution in the coastal environment. A review.* Journal of Materials and Environmental Science, 2018. **9**(4): p. 1170-1181.
66. Li, J., A.L. Lusher, J.M. Rotchell, S. Deudero, A. Turra, I.L.N. Bråte, C. Sun, M. Shahadat Hossain, et al., *Using mussel as a global bioindicator of coastal microplastic pollution.* Environmental Pollution, 2019. **244**: p. 522-533.
67. Kazour, M. and R. Amara, *Is blue mussel caging an efficient method for monitoring environmental microplastics pollution?* Science of The Total Environment, 2020. **710**: p. 135649.
68. Voudanta, E., K.A. Kormas, S. Monchy, A. Delegrange, D. Vincent, S. Genitsaris, and U. Christaki, *Mussel biofiltration effects on attached bacteria and unicellular eukaryotes in fish-rearing seawater.* PeerJ, 2016. **4**: p. e1829.
69. Paul-Pont, I., K. Tallec, C. Gonzalez-Fernandez, C. Lambert, D. Vincent, D. Mazurais, J.-L. Zambonino-Infante, G. Brotons, et al., *Constraints and Priorities for Conducting Experimental Exposures of Marine Organisms to Microplastics.* Frontiers in Marine Science, 2018. **5**: p. 252.
70. Bour, A., A. Haarr, S. Keiter, and K. Hylland, *Environmentally relevant microplastic exposure affects sediment-dwelling bivalves.* Environmental Pollution, 2018. **236**: p. 652-660.
71. Dayras, P., C. Bialais, J.-S. Lee, and S. Souissi, *Effects of microalgal diet on the population growth and fecundity of the cyclopoid copepod Paracyclopina nana.* Journal of the World Aquaculture Society, 2020. **n/a**(n/a): p. 1-16.
72. Lee, R., A. Lovatelli, and L. Ababouch, *Bivalve depuration: fundamental and practical aspects*. FAO Fisheries Technical Paper. No. 511. 2008, Rome: Food and Agriculture Organization of The United Nations.
73. Kozich, J.J., S.L. Westcott, N.T. Baxter, S.K. Highlander, and P.D. Schloss, *Development of a Dual-Index Sequencing Strategy and Curation Pipeline for Analyzing Amplicon Sequence Data on the MiSeq Illumina Sequencing Platform.* Applied and Environmental Microbiology, 2013. **79**(17): p. 5112.
74. Schloss, P.D., D. Gevers, and S.L. Westcott, *Reducing the Effects of PCR Amplification and Sequencing Artifacts on 16S rRNA-Based Studies.* PLoS ONE, 2011. **6**(12): p. e27310.
75. Quast, C., E. Pruesse, P. Yilmaz, J. Gerken, T. Schweer, P. Yarza, J. Peplies, and F.O. Glockner, *The SILVA ribosomal RNA gene database project: improved data processing and web-based tools.* Nucleic Acids Res, 2013. **41**(Database issue): p. D590-6.
76. Edgar, R.C., *Search and clustering orders of magnitude faster than BLAST.* Bioinformatics, 2010. **26**(19): p. 2460-2461.
77. Behnke, A., M. Engel, R. Christen, M. Nebel, R.R. Klein, and T. Stoeck, *Depicting more accurate pictures of protistan community complexity using pyrosequencing of hypervariable SSU rRNA gene regions.* Environmental Microbiology, 2011. **13**(2): p. 340-349.
78. Kunin, V., A. Engelbrektson, H. Ochman, and P. Hugenholtz, *Wrinkles in the rare biosphere: pyrosequencing errors can lead to artificial inflation of diversity estimates.* Environmental Microbiology, 2010. **12**(1): p. 118-123.

79. Altschul, S.F., W. Gish, W. Miller, E.W. Myers, and D.J. Lipman, *Basic local alignment search tool.* Journal of Molecular Biology, 1990. **215**(3): p. 403-410.
80. Hammer, O., D. Harper, and P. Ryan, *PAST: Paleontological Statistics Software Package for Education and Data Analysis.* Palaeontologia Electronica, 2001. **4**: p. 1-9.
81. Pinheiro, J., D. Bates, S. DebRoy, D. Sarkar, and R.C. Team, *nlme: Linear and Nonlinear Mixed Effects Models. R package version 3.1-148*. 2020.
82. Clarke, K.R. and R.N. Gorley, *Primer V6: User Manual - Tutorial*. 2006, Plymouth, UK: Plymouth Marine Laboratory.
83. Oksanen, J., F.G. Blanchet, M. Friendly, R. Kindt, P. Legendre, D. McGlinn, P.R. Minchin, R.B. O'Hara, et al., *vegan: Community Ecology Package. R package version 2.5-6*. 2019.
84. Segata, N., J. Izard, L. Waldron, D. Gevers, L. Miropolsky, W.S. Garrett, and C. Huttenhower, *Metagenomic biomarker discovery and explanation.* Genome Biology, 2011. **12**(6): p. R60.
85. Cáceres, M.D. and P. Legendre, *Associations between species and groups of sites: indices and statistical inference.* Ecology, 2009. **90**(12): p. 3566-3574.
86. Langille, M.G.I., J. Zaneveld, J.G. Caporaso, D. McDonald, D. Knights, J.A. Reyes, J.C. Clemente, D.E. Burkepile, et al., *Predictive functional profiling of microbial communities using 16S rRNA marker gene sequences.* Nature Biotechnology, 2013. **31**(9): p. 814-821.
87. Norén, F., *Small plastic particles in Coastal Swedish waters*, S. N-research Marine Consulting, Editor. 2007, KIMO (Kommunenes Internasjonale Miljøorganisasjon) Sweden: Gothenburg.
88. Kane, I.A., M.A. Clare, E. Miramontes, R. Wogelius, J.J. Rothwell, P. Garreau, and F. Pohl, *Seafloor microplastic hotspots controlled by deep-sea circulation.* Science, 2020: p. eaba5899.
89. Conkle, J.L., C.D. Baez Del Valle, and J.W. Turner, *Are We Underestimating Microplastic Contamination in Aquatic Environments?* Environmental Management, 2018. **61**(1): p. 1-8.
90. Lindeque, P.K., M. Cole, R.L. Coppock, C.N. Lewis, R.Z. Miller, A.J.R. Watts, A. Wilson-McNeal, S.L. Wright, et al., *Are we underestimating microplastic abundance in the marine environment? A comparison of microplastic capture with nets of different mesh-size.* Environmental Pollution, 2020: p. 114721.
91. Lozano, R.L. and J. Mouat, *Marine litter in the North-East Atlantic Region: Assessment and priorities for response*. OSPAR 2009: London, United Kingdom.
92. Cai, M., H. He, M. Liu, S. Li, G. Tang, W. Wang, P. Huang, G. Wei, et al., *Lost but can't be neglected: Huge quantities of small microplastics hide in the South China Sea.* Science of The Total Environment, 2018. **633**: p. 1206-1216.
93. Liu, P., X. Zhan, X. Wu, J. Li, H. Wang, and S. Gao, *Effect of weathering on environmental behavior of microplastics: Properties, sorption and potential risks.* Chemosphere, 2020. **242**: p. 125193.
94. Luo, H., Y. Zhao, Y. Li, Y. Xiang, D. He, and X. Pan, *Aging of microplastics affects their surface properties, thermal decomposition, additives leaching and interactions in simulated fluids.* Science of The Total Environment, 2020. **714**: p. 136862.
95. Rummel, C.D., A. Jahnke, E. Gorokhova, D. Kühnel, and M. Schmitt-Jansen, *Impacts of Biofilm Formation on the Fate and Potential Effects of Microplastic in the Aquatic Environment.* Environmental Science & Technology Letters, 2017. **4**(7): p. 258-267.
96. Vroom, R.J.E., A.A. Koelmans, E. Besseling, and C. Halsband, *Aging of microplastics promotes their ingestion by marine zooplankton.* Environmental Pollution, 2017. **231**(Pt 1): p. 987-996.
97. Chen, X., X. Xiong, X. Jiang, H. Shi, and C. Wu, *Sinking of floating plastic debris caused by biofilm development in a freshwater lake.* Chemosphere, 2019. **222**: p. 856-864.
98. Nguyen, T.H., F.H.M. Tang, and F. Maggi, *Sinking of microbial-associated microplastics in natural waters.* PLOS ONE, 2020. **15**(2): p. e0228209.
99. Kothary, M.H. and U.S. Babu, *Infective dose of foodborne pathogens in volunteers: a review.* Journal of Food Safety, 2001. **21**(1): p. 49-68.

100. Koehler, A., A. Anderson, A. Andrady, C. Arthur, J. Baker, H. Bouwman, S. Gall, V. Hidalgo-Ruz, et al., *Sources, fate and effects of microplastics in the marine environment: a global assessment*. IMO/FAO/UNESCO-IOC/UNIDO/WMO/IAEA/UN/UNEP/UNDP Joint Group of Experts on the Scientific Aspects of Marine Environmental Protection, ed. P. Kershaw. 2015, London, UK: International Maritime Organization.
101. Girbau, C., I. Martinez-Malaxetxebarria, G. Muruaga, S. Carmona, R. Alonso, and A. Fernandez-Astorga, *Study of Biofilm Formation Ability of Foodborne Arcobacter butzleri under Different Conditions.* Journal of Food Protection, 2017. **80**(5): p. 758-762.
102. Yin, W., Y. Wang, L. Liu, and J. He, *Biofilms: The Microbial "Protective Clothing" in Extreme Environments.* International journal of molecular sciences, 2019. **20**(14): p. 3423.
103. Lee, J.-W., J.-H. Nam, Y.-H. Kim, K.-H. Lee, and D.-H. Lee, *Bacterial communities in the initial stage of marine biofilm formation on artificial surfaces.* The Journal of Microbiology, 2008. **46**(2): p. 174-182.
104. Koedooder, C., W. Stock, A. Willems, S. Mangelinckx, M. De Troch, W. Vyverman, and K. Sabbe, *Diatom-Bacteria Interactions Modulate the Composition and Productivity of Benthic Diatom Biofilms.* Frontiers in Microbiology, 2019. **10**: p. 1255.
105. Op den Camp, H.J.M., M.S.M. Jetten, and M. Strous, *Chapter 16 - Anammox*, in *Biology of the Nitrogen Cycle*, H. Bothe, S.J. Ferguson, and W.E. Newton, Editors. 2007, Elsevier: Amsterdam. p. 245-262.
106. Zhao, J.-S., D. Manno, and J. Hawari, *Psychrilyobacter atlanticus gen. nov., sp. nov., a marine member of the phylum Fusobacteria that produces H2 and degrades nitramine explosives under low temperature conditions.* International Journal of Systematic and Evolutionary Microbiology, 2009. **59**(3): p. 491-497.
107. Shahinpei, A., M.A. Amoozegar, S.A.S. Fazeli, P. Schumann, and A. Ventosa, *Salinispirillum marinum gen. nov., sp. nov., a haloalkaliphilic bacterium in the family 'Saccharospirillaceae'.* International Journal of Systematic and Evolutionary Microbiology, 2014. **64**(11): p. 3610-3615.
108. Castelle, C.J. and J.F. Banfield, *Major New Microbial Groups Expand Diversity and Alter our Understanding of the Tree of Life.* Cell, 2018. **172**(6): p. 1181-1197.
109. Liu, J., Y. Wang, Y. Liu, and X.-H. Zhang, *Ahrensia marina sp. nov., a dimethylsulfoniopropionate-cleaving bacterium isolated from seawater, and emended descriptions of the genus Ahrensia and Ahrensia kielensis.* International Journal of Systematic and Evolutionary Microbiology, 2016. **66**(2): p. 874-880.
110. Asami, H., M. Aida, and K. Watanabe, *Accelerated Sulfur Cycle in Coastal Marine Sediment beneath Areas of Intensive Shellfish Aquaculture.* Applied and Environmental Microbiology, 2005. **71**(6): p. 2925.
111. Buchan, A., G.R. LeCleir, C.A. Gulvik, and J.M. González, *Master recyclers: features and functions of bacteria associated with phytoplankton blooms.* Nature Reviews Microbiology, 2014. **12**(10): p. 686-698.
112. Yeats, R.B., *Monoterpenoids*, in *Terpenoids and Steroids: Volume 6*, K.H. Overton, Editor. 1976, The Royal Society of Chemistry. p. 1-51.
113. Tinge, J., M. Groothaert, H. op het Veld, J. Ritz, H. Fuchs, H. Kieczka, and W.C. Moran, *Caprolactam.* Ullmann's Encyclopedia of Industrial Chemistry, 2018: p. 1-31.
114. Rossberg, M., W. Lendle, G. Pfleiderer, A. Tögel, E.-L. Dreher, E. Langer, H. Rassaerts, P. Kleinschmidt, et al., *Chlorinated Hydrocarbons.* Ullmann's Encyclopedia of Industrial Chemistry, 2006.

115. Wieczorek, A.M., P.L. Croot, F. Lombard, J.N. Sheahan, and T.K. Doyle, *Microplastic Ingestion by Gelatinous Zooplankton May Lower Efficiency of the Biological Pump.* Environmental Science & Technology, 2019. **53**(9): p. 5387-5395.

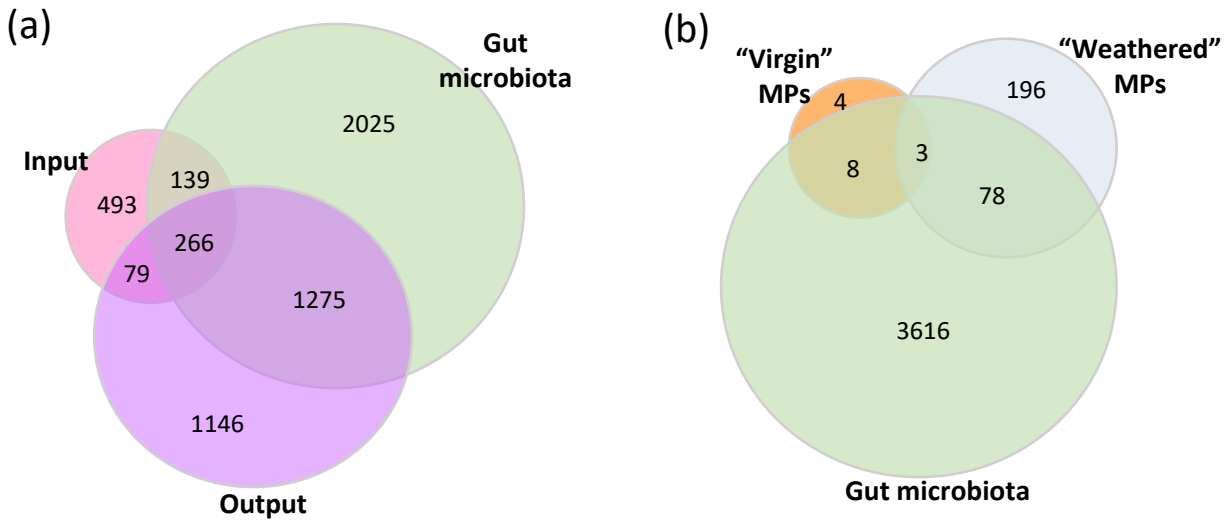

Figure 1. 16S rRNA gene sequences analysis. Operational taxonomic units (OTUs) shared among different sample groups. (a) OTUs shared among input microbiota (filtered seawater, virgin MPs, and weathered MPs), mussel gut microbiota, and output microbiota (feces/tank water). (b) OTUs shared among "virgin" MPs microbiota, "weathered" MPs microbiota, and mussel gut microbiota.

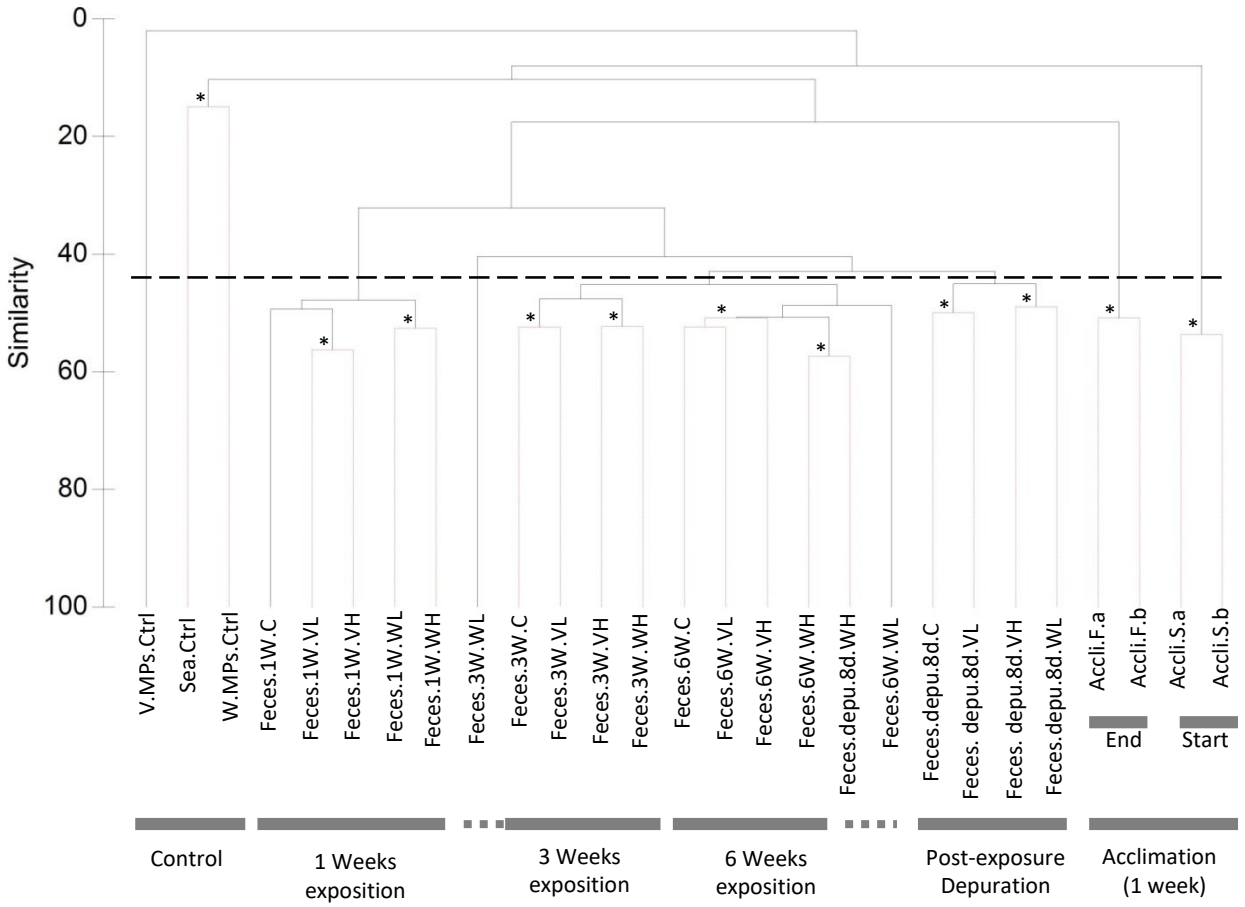

Figure 2. Hierarchical clustering of control and tank water/feces microbial diversity based on Bray–Curtis dissimilarities calculated on double square root transformed number of OTUs reads. "*" in the dendrogram indicate similarities between bifurcations/samples, based on the SIMPROF significance test. The dash line indicate arbitrary cluster separation, while solid lines on the bottom represent cluster separation according the sample origin. Abbreviations: 1W – 1-week; 3W – 3 weeks; 6W – 6 weeks; D2d – depuration 2-day; D8d – depuration 8-day; C – control; VL – virgin low; VH – virgin high; WL – weathered low; WH – weathered high.

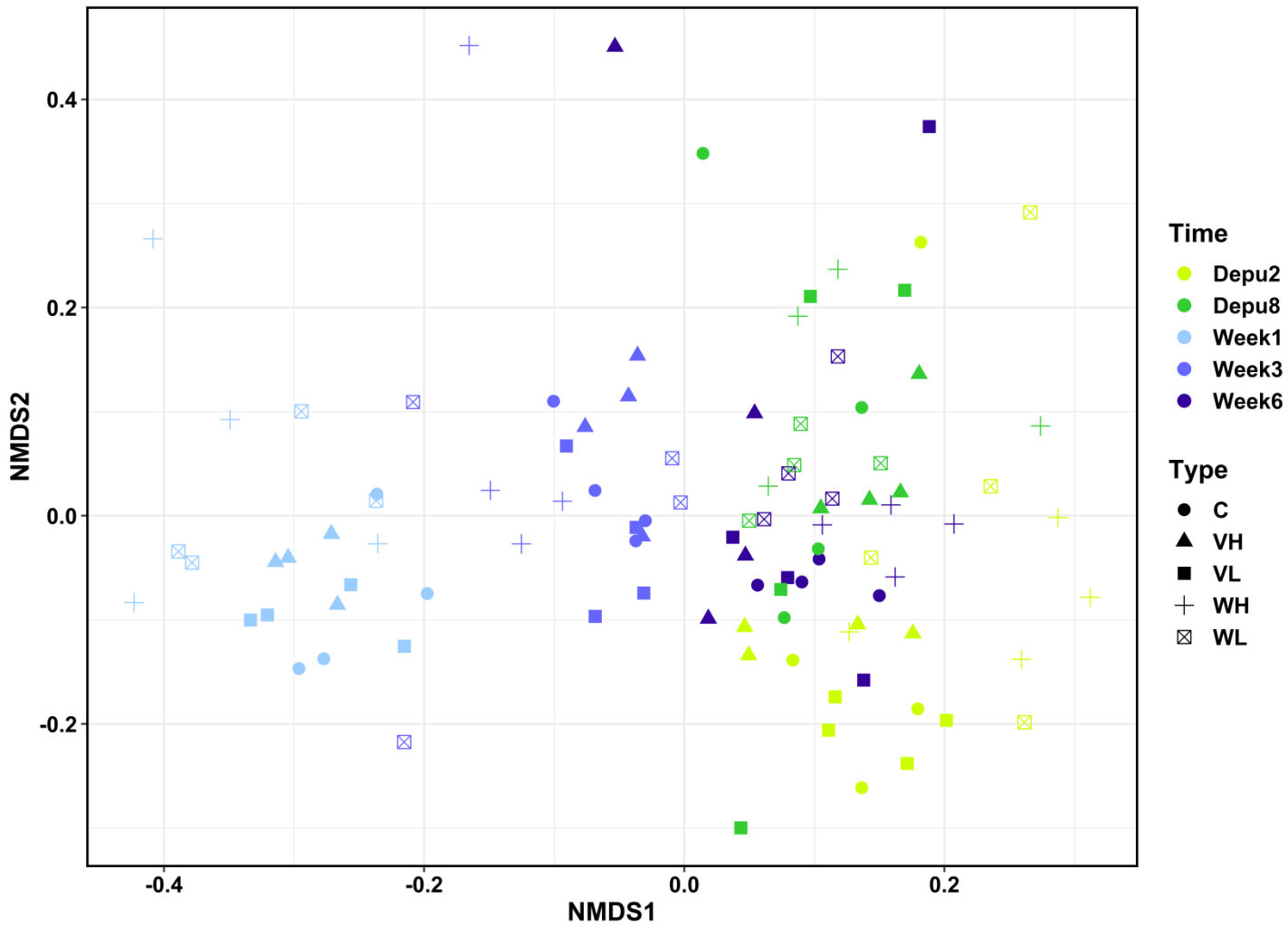

Figure 3. Non-metric multidimensional scaling (NMDS) on the gut microbiota community. The analysis was performed on the gut bacterial OTUs composition during the 6-week MPs exposure (1, 3 and 6 weeks) and depuration (2 and 8 days). Shapes of symbols correspond to different treatments and colors of symbols correspond to different time points. Abbreviations: C – control; VL – virgin low; VH – virgin high; WL – weathered low; WH – weathered high; "C": control without MPs; "VL": virgin MPs at low concentration; "VH": virgin MPs at high concentration; "WL": weathered MPs at low concentration; "WH": weathered MPs at high concentration; Depu2 – depuration 2-day; Depu8 – depuration 8-day.

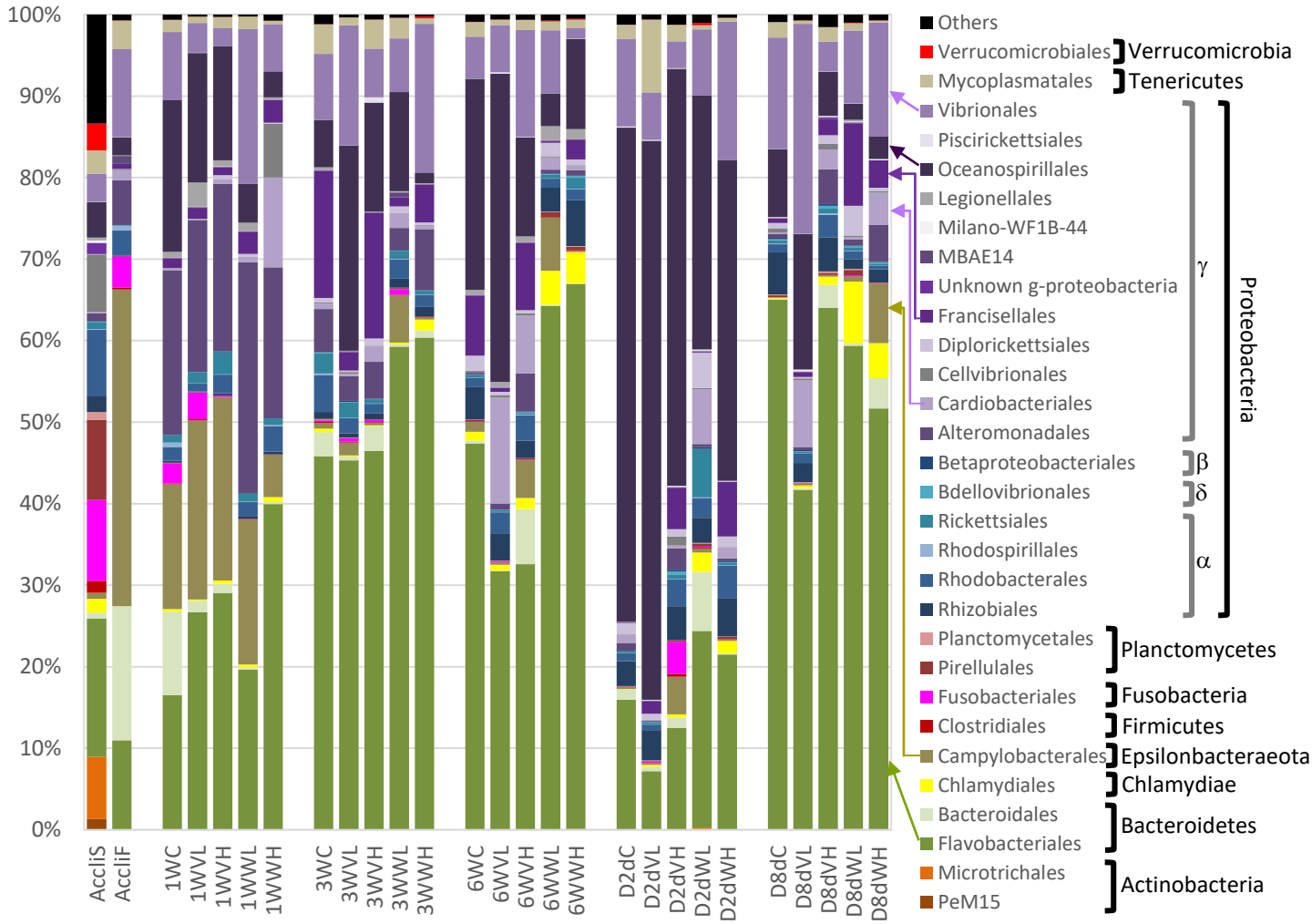

Figure 4. Microbial community composition of mussel gut microbiota (at order level). Taxa were grouped first by phylum then by class. Bacteroidetes was presented in shades of green; Chlamydiae was presented in yellow; α, δ, and β Proteobacteria were presented in shades of blue; γ Proteobacteria were presented in shades of purple. Taxa ratios in the community were detailed in Supplementary material 3. Abbreviations: Accli.S – acclimation start; Accli.F – acclimation finish; 1W – 1 week; 3W – 3 weeks; 6W – 6 weeks; D2d – depuration 2-day; D8d – depuration 8-day; C – control; VL – virgin low; VH – virgin high; WL – weathered low; WH – weathered high.

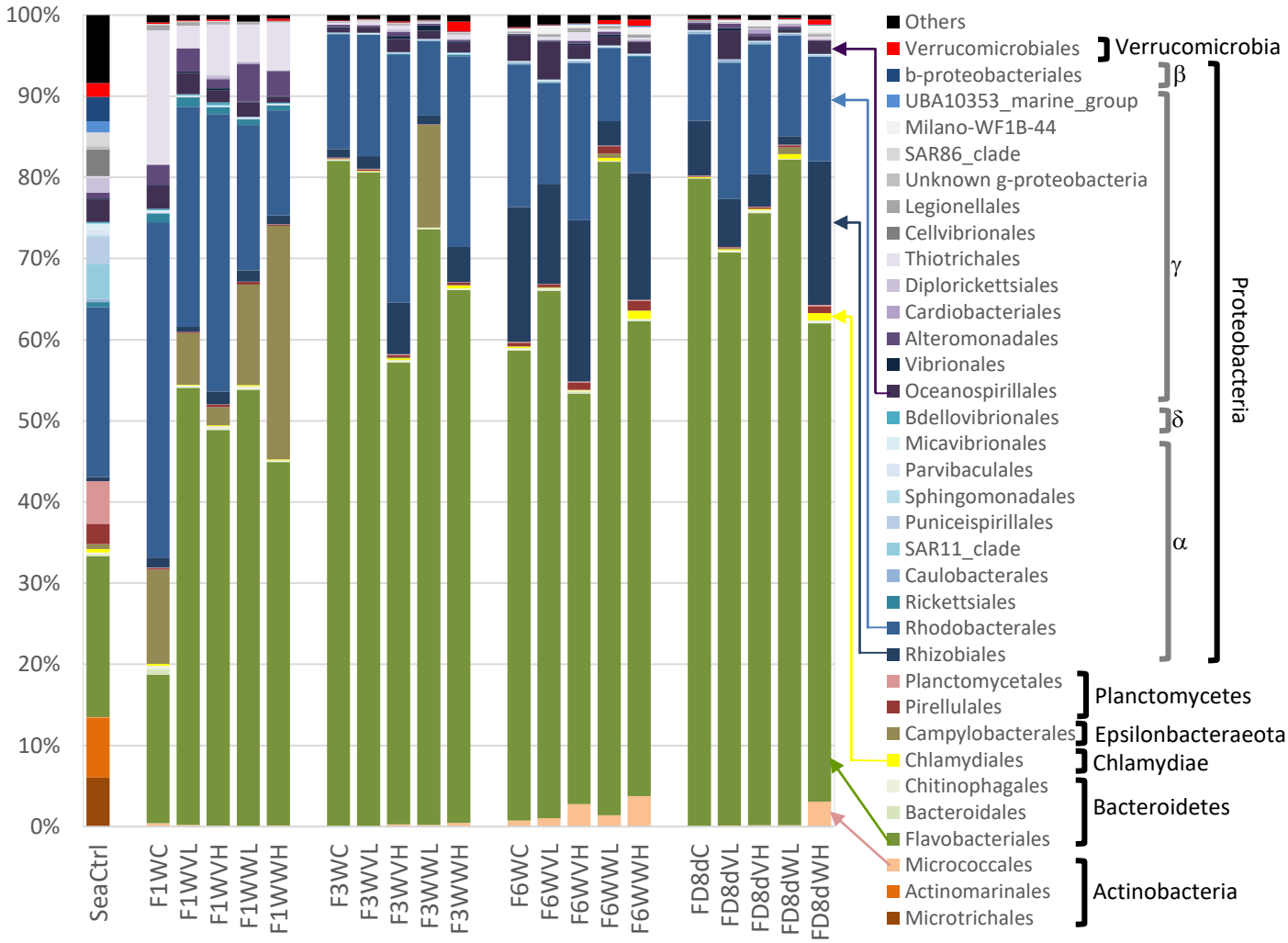

Figure 5. Microbial community composition of mussel feces and tank water (at order level). Taxa were grouped first by phylum then by class. Actinobacteria was presented in shades of orange; Bacteroidetes was presented in shades of green; Chlamydiae was presented in yellow; α, δ, and β Proteobacteria were presented in shades of blue; γ Proteobacteria were presented in shades of purple. Taxa ratios in the community were detailed in Supplementary material 4. Abbreviations: 1W – 1 week; 3W – 3 weeks; 6W – 6 weeks; D8d – depuration 8-day; C – control; VL – virgin low; VH – virgin high; WL – weathered low; WH – weathered high.

(a) OTUs with decreased abundance

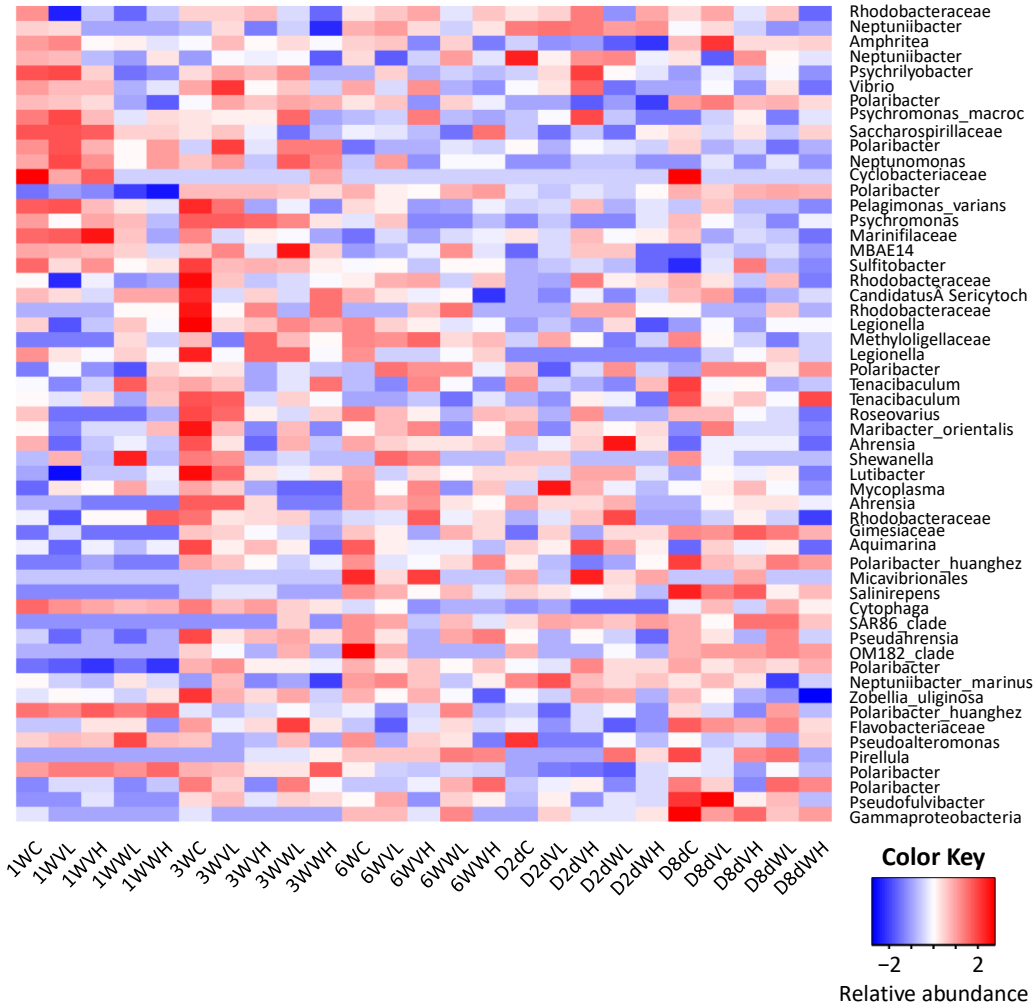

Figure 6. OTUs that have significant difference in abundance in MPs exposed samples as compared with the control. (a) OTUs (as shown in their taxa) with decreased abundance. (b) OTUs with increased abundance. Identification of OTUs (including accession number) and information of significant changes were detailed in Supplementary material 5. Abbreviations: 1W – 1-week; 3W – 3 weeks; 6W – 6 weeks; D2d – depuration 2-day; D8d – depuration 8-day; C – control; VL – virgin low; VH – virgin high; WL – weathered low; WH – weathered high.

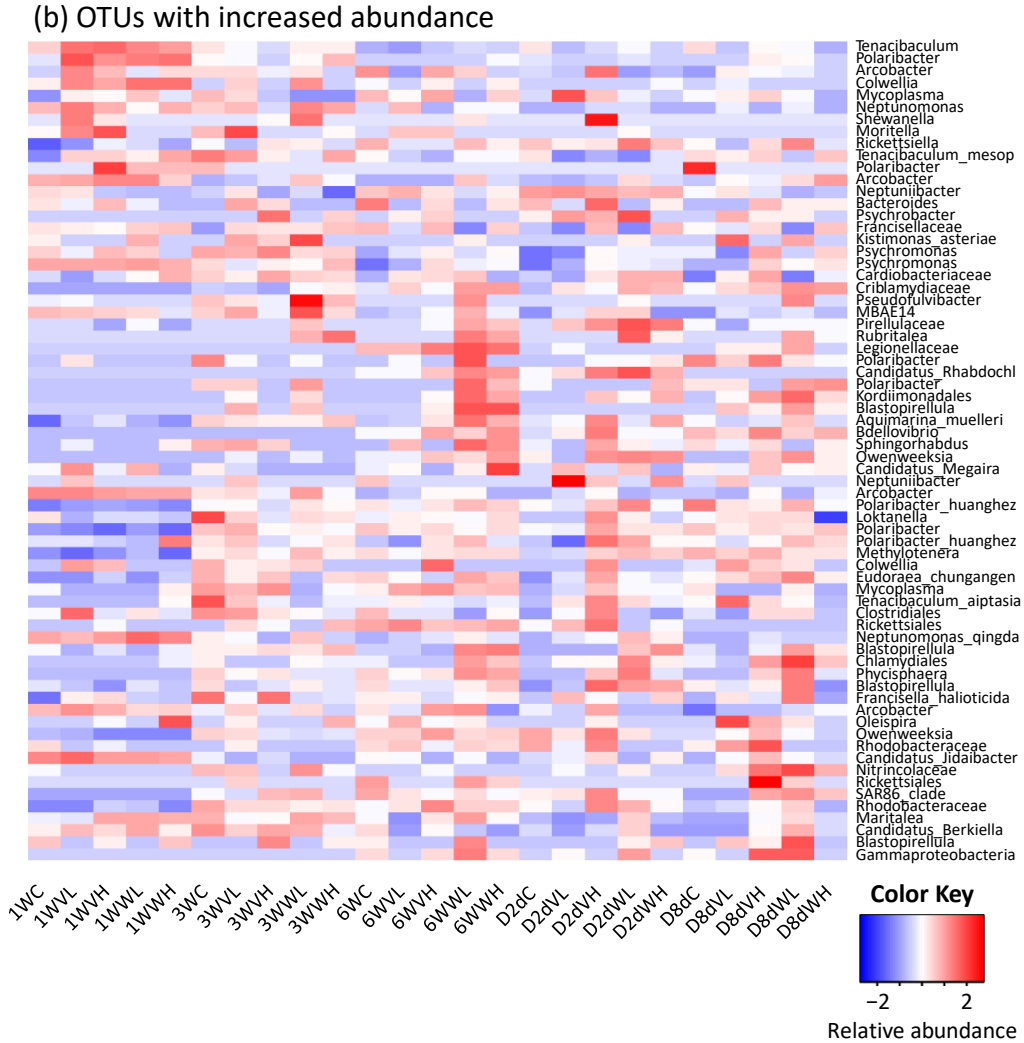

Figure 6. OTUs that have significant difference in abundance in MPs exposed samples as compared with the control. (a) OTUs (as shown in their taxa) with decreased abundance. (b) OTUs with increased abundance. Identification of OTUs (including accession number) and information of significant changes were detailed in Supplementary material 5. Abbreviations: 1W – 1-week; 3W – 3 weeks; 6W – 6 weeks; D2d – depuration 2-day; D8d – depuration 8-day; C – control; VL – virgin low; VH – virgin high; WL – weathered low; WH – weathered high.

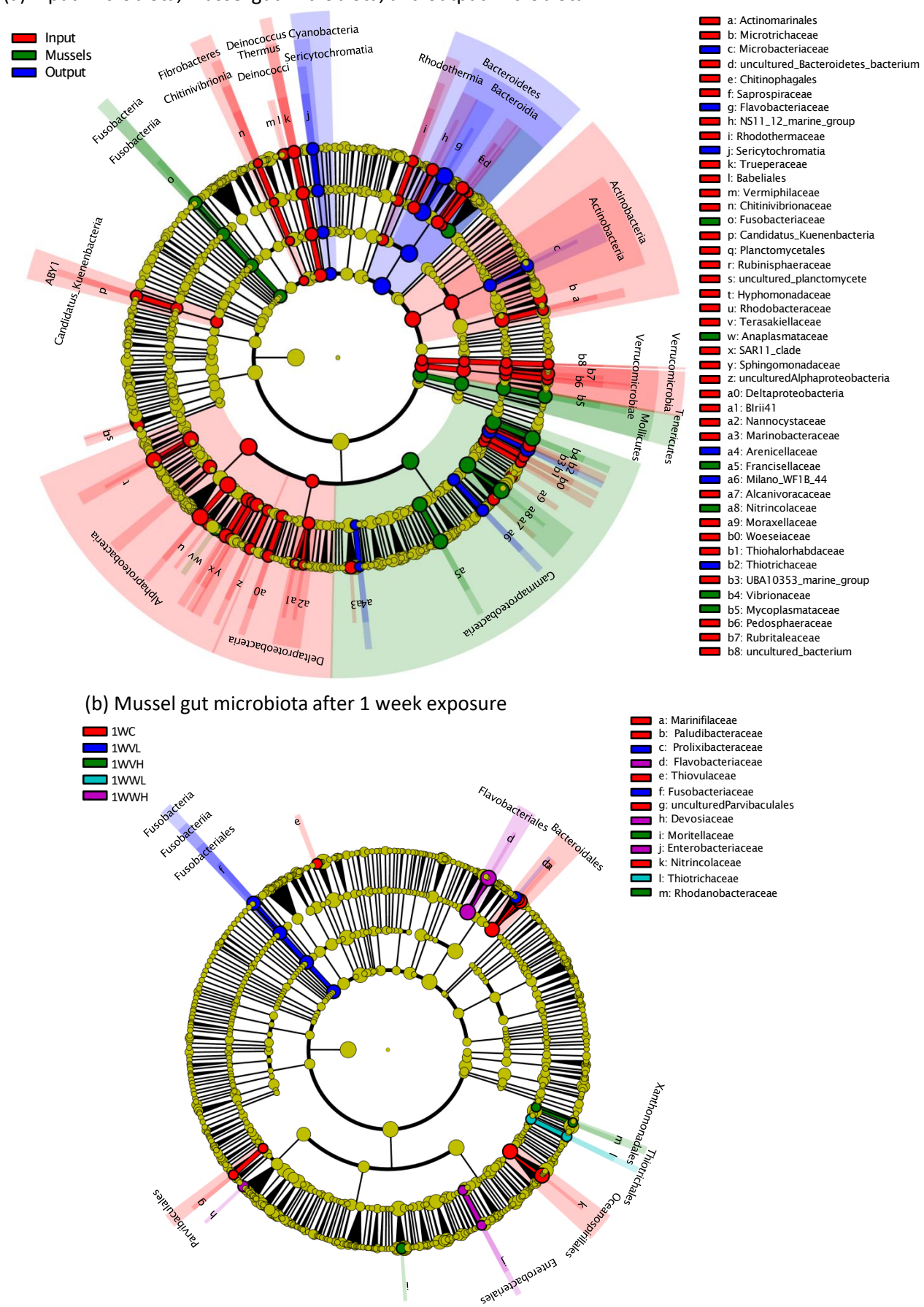

Figure 7. Linear discriminant analysis effect size (LEfSe) for identifying potential unique biomarkers in each sample group. (a) Sample groups: input microbiota, mussel gut microbiota, and output microbiota. (b) Mussel gut microbiota after 1 week exposure, (c) Mussel gut microbiota after 3 weeks exposure, (d) Mussel gut microbiota after 6 weeks exposure, (e) Mussel gut microbiota after 2 days depuration, (f) Mussel gut microbiota after 8 days depuration. Details were listed in Supplementary material 7.

(c) Mussel gut microbiota after 3 weeks exposure

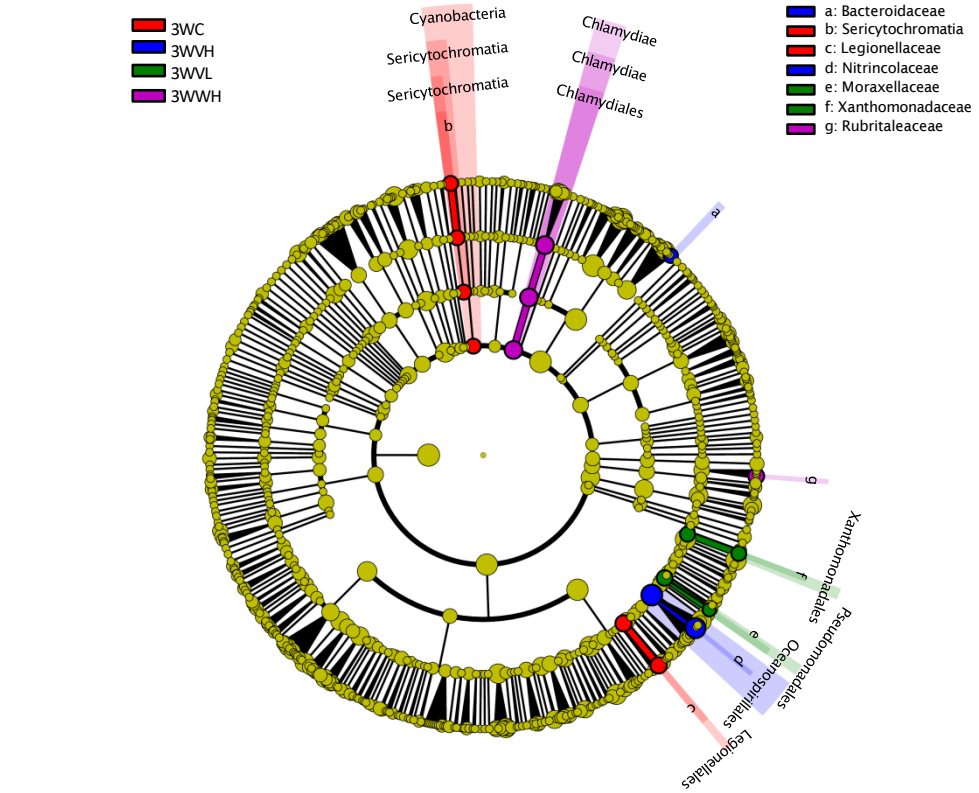

(d) Mussel gut microbiota after 6 weeks exposure

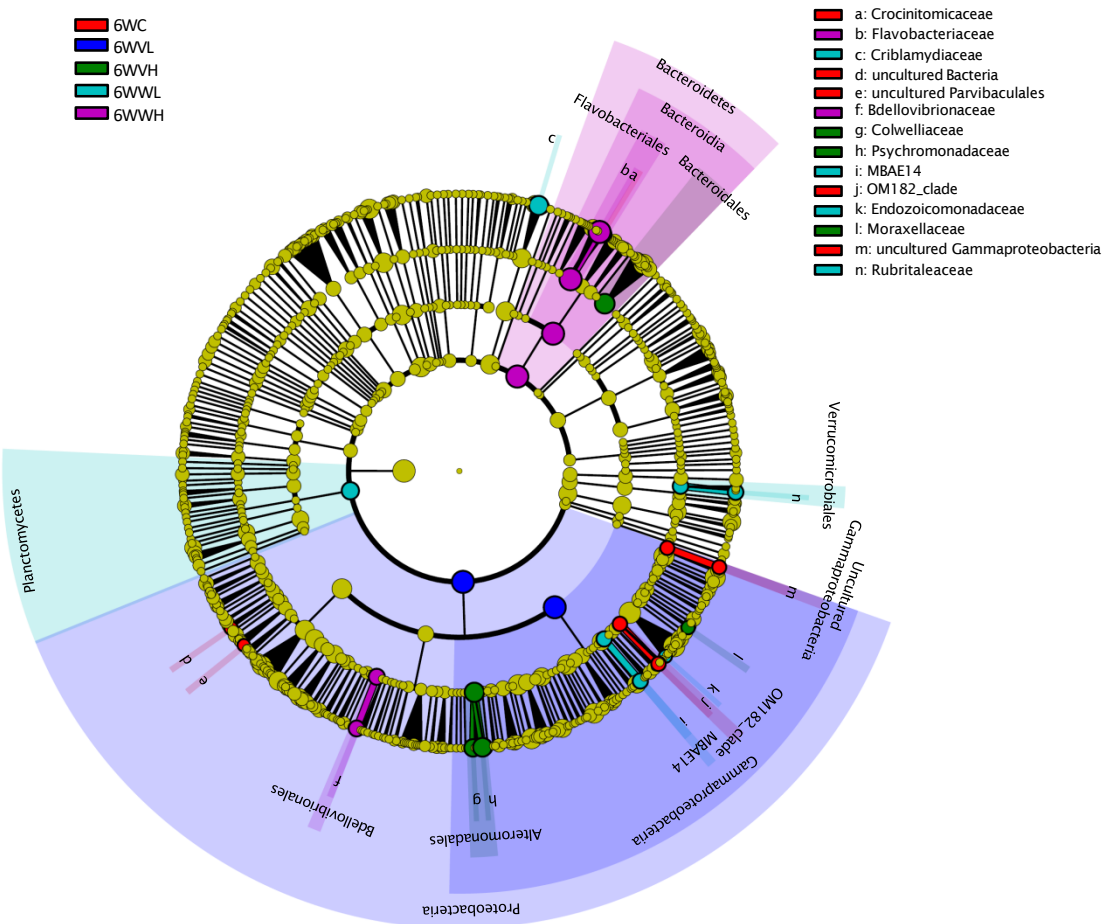

Figure 7. Linear discriminant analysis effect size (LEfSe) for identifying potential unique biomarkers in each sample group. (a) Sample groups: input microbiota, mussel gut microbiota, and output microbiota. (b) Mussel gut microbiota after 1 week exposure, (c) Mussel gut microbiota after 3 weeks exposure, (d) Mussel gut microbiota after 6 weeks exposure, (e) Mussel gut microbiota after 2 days depuration, (f) Mussel gut microbiota after 8 days depuration. Details were listed in Supplementary material 7.

(e) Mussel gut microbiota after 2 days depuration

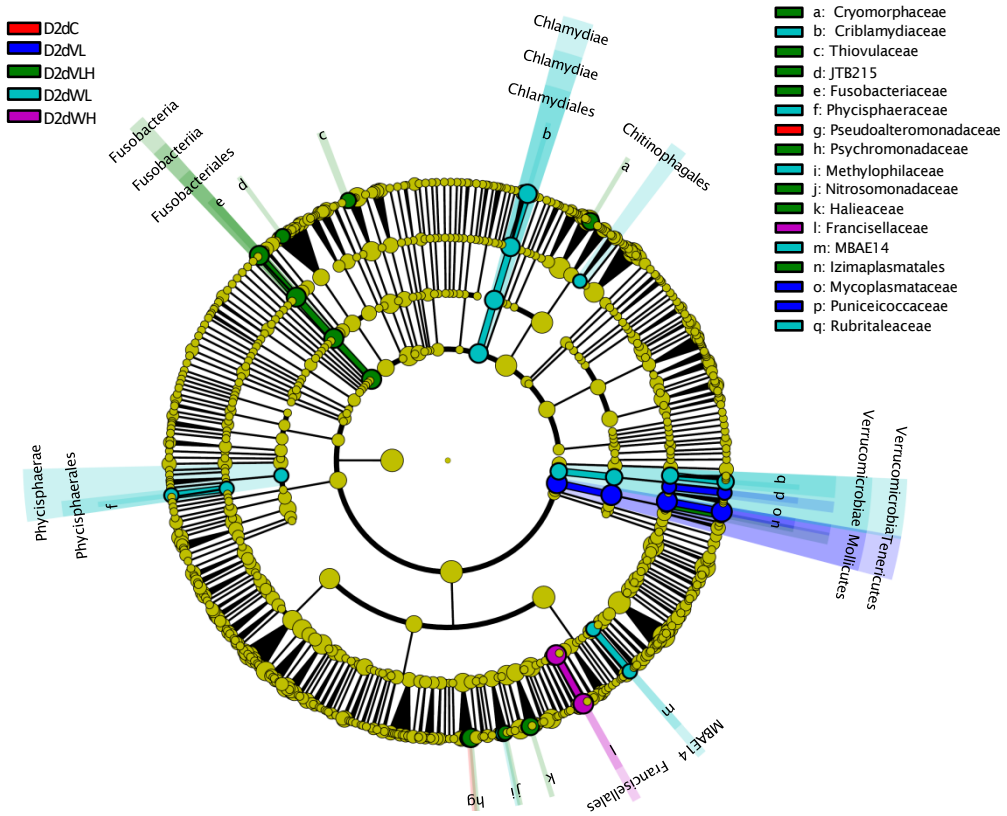

(f) Mussel gut microbiota after 8 days depuration

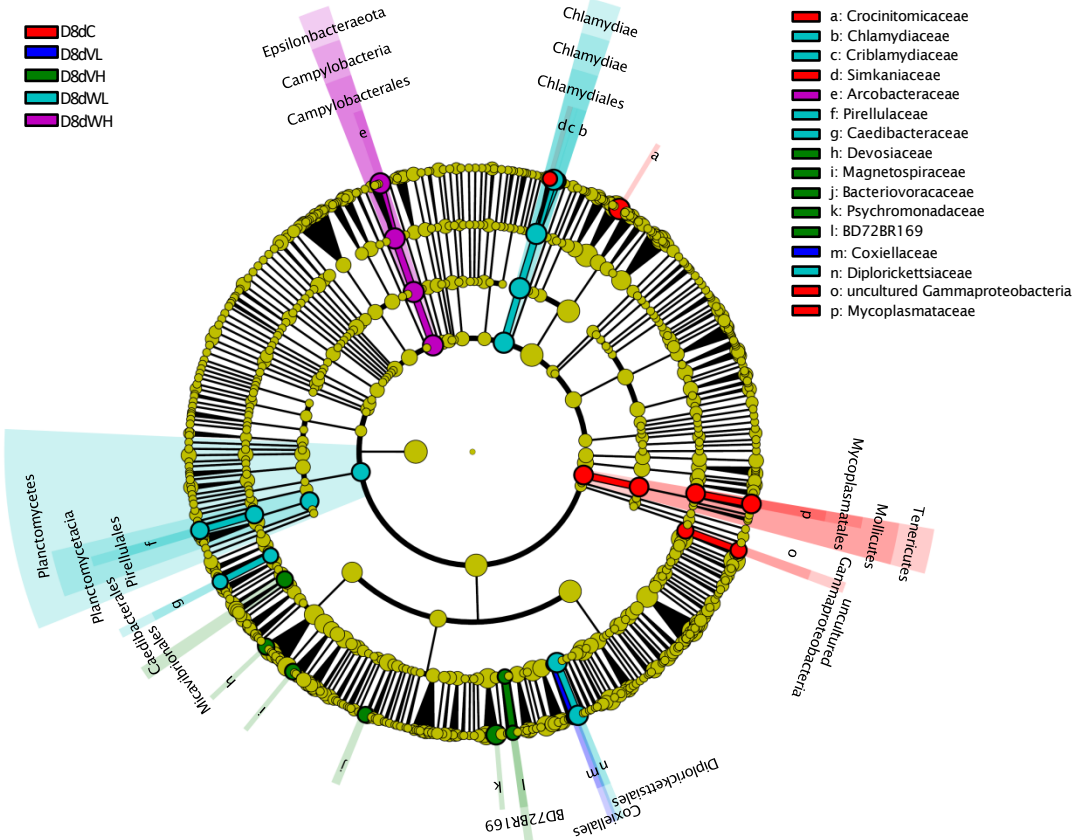

Figure 7. Linear discriminant analysis effect size (LEfSe) for identifying potential unique biomarkers in each sample group. (a) Sample groups: input microbiota, mussel gut microbiota, and output microbiota. (b) Mussel gut microbiota after 1 week exposure, (c) Mussel gut microbiota after 3 weeks exposure, (d) Mussel gut microbiota after 6 weeks exposure, (e) Mussel gut microbiota after 2 days depuration, (f) Mussel gut microbiota after 8 days depuration. Details were listed in Supplementary material 7.

Figure captions

Fig.1(A-D) (A) Chemical structure of Eu(III)-CPLx with CHN elemental analysis, (B&C) ^{1}H NMR (500 MHz, $CDCl_3$) spectra of 5,5'-DMBP and phen and (D) ^{1}H NMR (500 MHz, CD_3OD) spectrum of Eu(III)-CPLx.

Fig.2(A-D) (A) FT-IR spectra of (a) 5,5'-DMBP, (b) phen, (c) Eu(III)-CPLx and (d) fluorescent Eu(III)-CPLx/D-Dex composite, (B) UV-visible spectra of (a) 5,5'-DMBP, (b) phen, (c) Eu(III)-CPLx and (d) fluorescent Eu(III)-CPLx/D-Dex composite, (C) Fluorescence spectra of (a) Eu(III)-CPLx and (b) fluorescent Eu(III)-CPLx/D-Dex composite and (D) X-ray diffraction spectra of (a) Eu(III)-CPLx and (b) fluorescent Eu(III)-CPLx/D-Dex composite.

Fig.3(A-D) (A) Commission international de l'éclairage (CIE) 1931 (x,y) color coordinates diagram of Eu(III)-CPLx (Yellow circle) and fluorescent Eu(III)-CPLx/D-Dex composite (Yellow square), (B) Energy transfer diagram with process from ligand to Eu(III) ion in the Eu(III)-CPLx (left) and fluorescent Eu(III)-CPLx/D-Dex composite (right), (C) TGA and DTA spectra of Eu(III)-CPLx and (D) fluorescent Eu(III)-CPLx/D-Dex composite.

Fig.4A SEM images of Eu(III)-CPLx with different magnification of (a) 100 µm, (b) 50 µm, (c) 20 µm ,(d) 10 µm and (e) EDAX analysis.

Fig.4B SEM images of fluorescent Eu(III)-CPLx/D-Dex composite with different magnification of (a) 200 µM, (b) 100 µM, (c) 50 µM ,(d) 20 µM and (e) 10 µM.

Fig.4C Elemental mapping of fluorescent Eu(III)-CPLx/D-Dex composite of (a) SEM image at 10 um, (b) C, (c) O (d) N (e) Eu.

Fig.5 LFP images developed with Eu(III)-CPLx on (a, a′) glass slide, (c, c′) aluminum foil, (e, e′) aluminum sheet (g, g′) aluminum rod under daylight and UV light at 365 nm and LFP images developed with fluorescent Eu(III)-CPLx/D-Dex composite on (b, b′) glass slide, (d, d′) aluminum foil, (f, f′) aluminum sheet (h,h′) aluminum rod under day light and UV light at 365 nm.

Fig.6 LFP images ridge details after developing on aluminum sheet substrate with fluorescent Eu(III)-CPLx/D-Dex composite including island, Fork, Lake, End ridge, Bifurcation, Pore, core and Eye under UV light irradiation at 365 nm.

Fig.7 LFP developed on aluminum sheet with Eu(III)-CPLx different aging (a) 0 day, (b) 1 week, (c) 2 week, (d) 3 week and (e) 4 week under UV light light irradiation at 365 nm and LFP developed on aluminum sheet with fluorescent Eu(III)-CPLx/D-Dex composite different aging (a) 0 day, (b) 1 week, (c) 2 week, (d) 3 week and (e) 4 week under UV light light irradiation at 365 nm.

Fig.8 LFP images developed by before and after abrasion on different substrates with Eu(III)-CPLx (a, a′) glass slide, (c, c′) aluminum foil, (e, e′) aluminum sheet (g, g′) aluminum rod under day light and UV light at 365 nm and LFP images developed by before and after abrasion on different substrates with fluorescent Eu(III)-CPLx/D-Dex composite on (b, b′) glass slide, (d, d′) aluminum foil, (f, f′) aluminum sheet (h,h′) aluminum rod under day light and UV light at 365 nm.

Fig.9(A-D) LFP detection different substrates with Eu(III)-CPLx and fluorescent Eu(III)-CPLx/D-Dex composite (A) (a, b)(d, e) plastic bottle lid (B) (a, b) (d, e) compact disc (C) (a, b)(d, e) glass beaker and (D) (a, b)(d, e) glass bottle under day light and UV-light irradiation at 365 nm. Expansion LFP image of (A) (c, f), plastic bottle lid (B) (c, f), compact disc (C) (c, f), glass beaker and (D) (c, f) glass bottle with Eu(III)-CPLx and fluorescent Eu(III)-CPLx/D-Dex composite under UV-light irradiation of 365 nm.

Fig.10 LFP images developed with Eu(III)-CPLx and fluorescent Eu(III)-CPLx/D-Dex composite on South Africa currency (a, d) under the normal light and 365 nm UV light irradiation (b, e) and expanded LFP image (c, f).

Fig.11(A-G) Comparison performance of LFP sweat pores by different labeling agents: (A) sky blue WBP 55G, (B) green BP 40G, (C) commercial ZnO powder, (D) Rhodamine 6G with day light, (E) Eu(III)-CPLx and (F) Fluorescent Eu(III)-CPLx/Dex composite under the UV light irradiation at 365 nm, (G) Calculate summarizing sweat pore.

Fig.12 (A-D) SEM images of LFP detection on aluminum sheet with Eu(III)-CPLx (A) 200 µM (B) 100 µM, (C) 50 µM and (D) 10 µM.

Fig.13 (A-D) SEM images of LFP detection on aluminum sheet with fluorescent Eu(III)-CPLx composite (A) 200 µM (B) 100 µM, (C) 50 µM and (D) 10 µM.

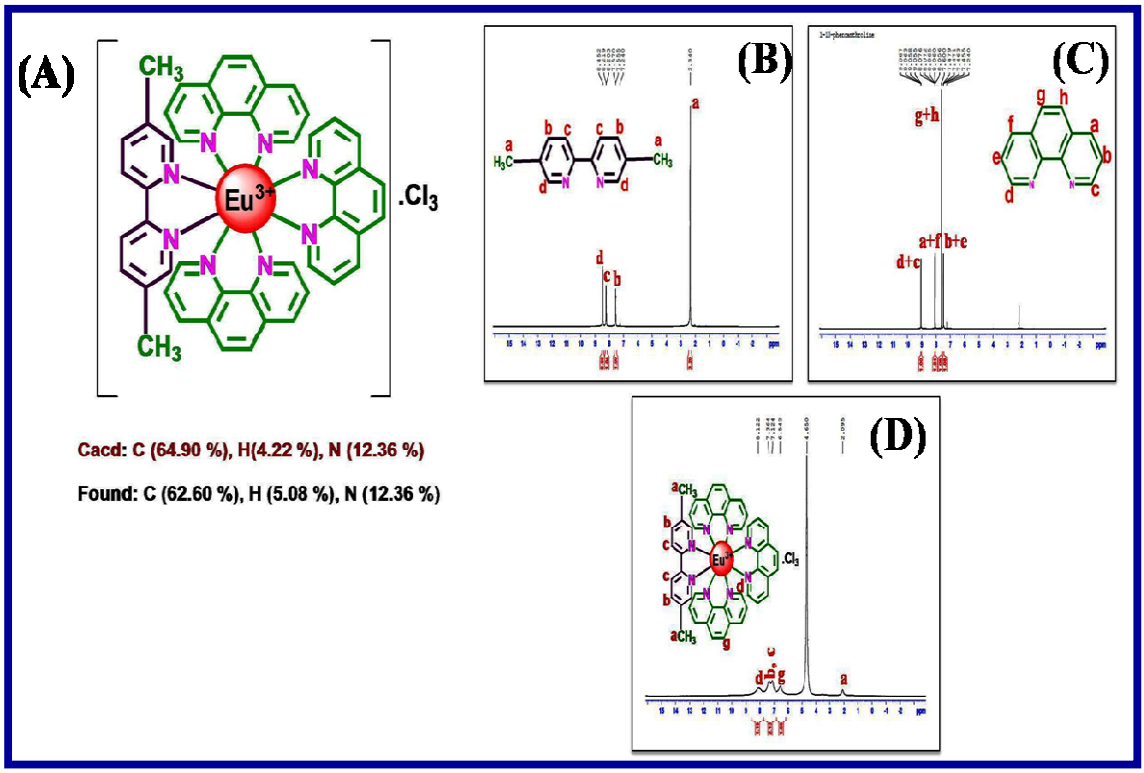

Fig.1(A-D) (A) Chemical structure of europium(III)complex with CHN elemental analysis (Calculated and Exp values), (B & C) ^{1}H NMR (500 MHz, $CDCl_3$) spectra of 5,5'-DMBP and phen and (D) 1H NMR (500 MHz, CD_3OD) spectrum of Eu(III)-CPLx.

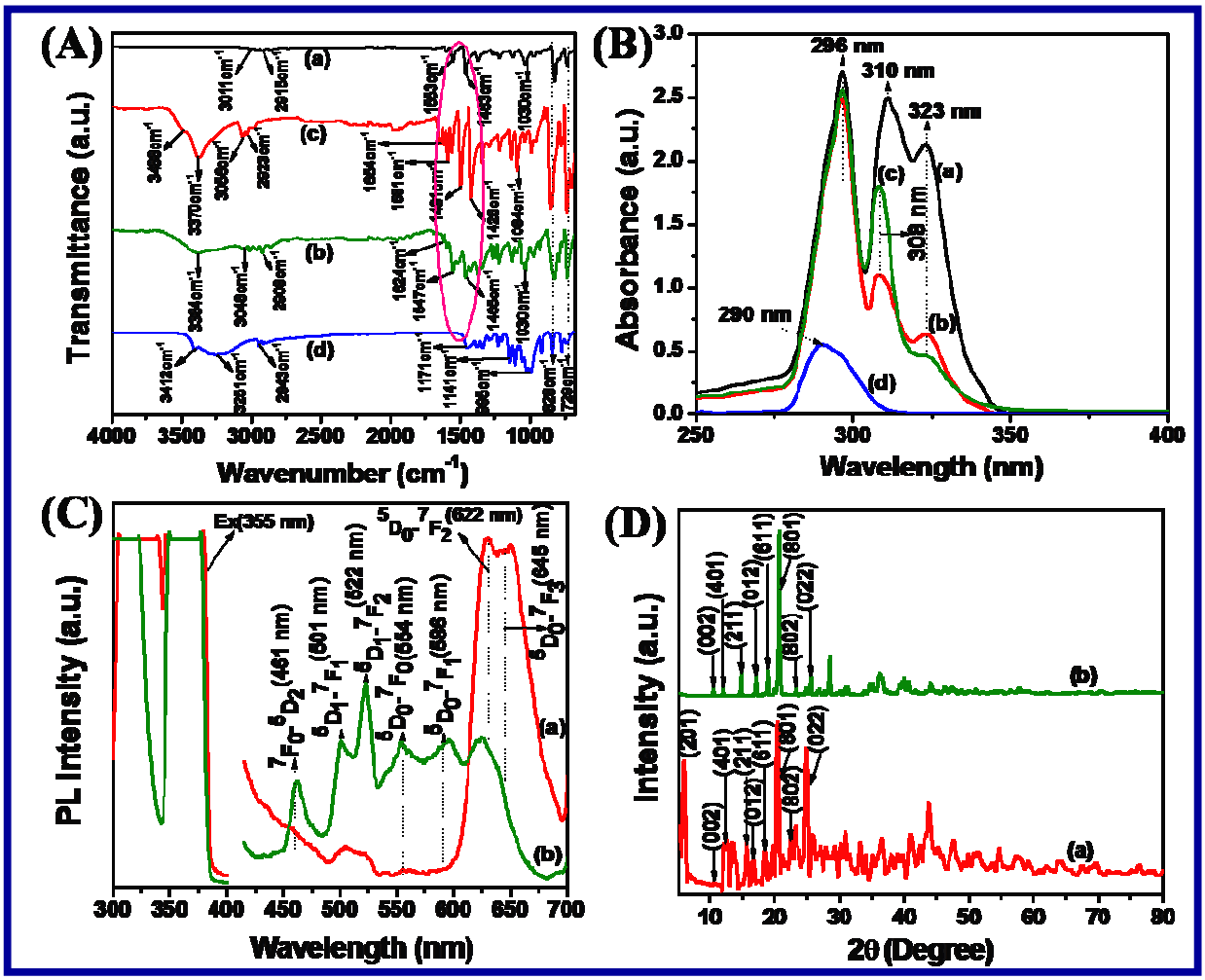

Fig.2(A-D) (A) FT-IR spectra of (a) 5,5'-DMBP, (b) phen, (c) Eu(III)-CPLx and (d) fluorescent Eu(III)-CPLx/D-Dex composite, (B) UV-visible spectra of (a) 5,5'-DMBP, (b) phen, (c) Eu(III)-CPLx and (d) fluorescent Eu(III)-CPLx/D-Dex composite, (C) Fluorescence spectra of (a) Eu(III)-CPLx and (b) fluorescent Eu(III)-CPLx/D-Dex composite and (D) X-ray diffraction spectra of (a) Eu(III)-CPLx and (b) fluorescent Eu(III)-CPLx/D-Dex composite.

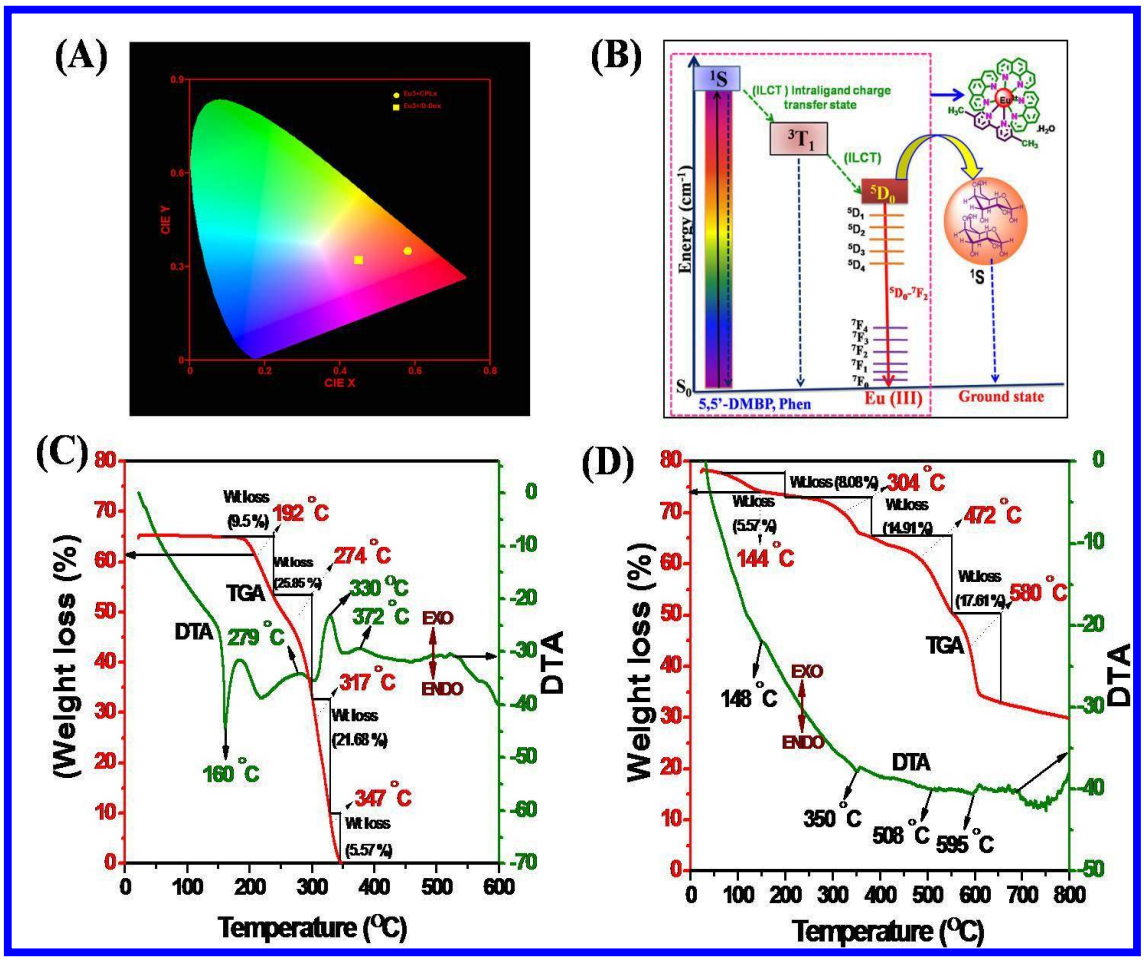

Fig.3(A-D) (A) Commission international de l'éclairage (CIE) 1931 (x,y) color coordinates diagram of Eu(III)-CPLx (Yellow circle) and fluorescent Eu(III)-CPLx/D-Dex composite (Yellow square), (B) Energy transfer diagram with process from ligand to Eu(III) ion in the Eu(III)-CPLx (left) and fluorescent Eu(III)-CPLx/D-Dex composite (right), (C) TGA and DTA spectra of Eu(III)-CPLx and (D) fluorescent Eu(III)-CPLx/D-Dex composite.

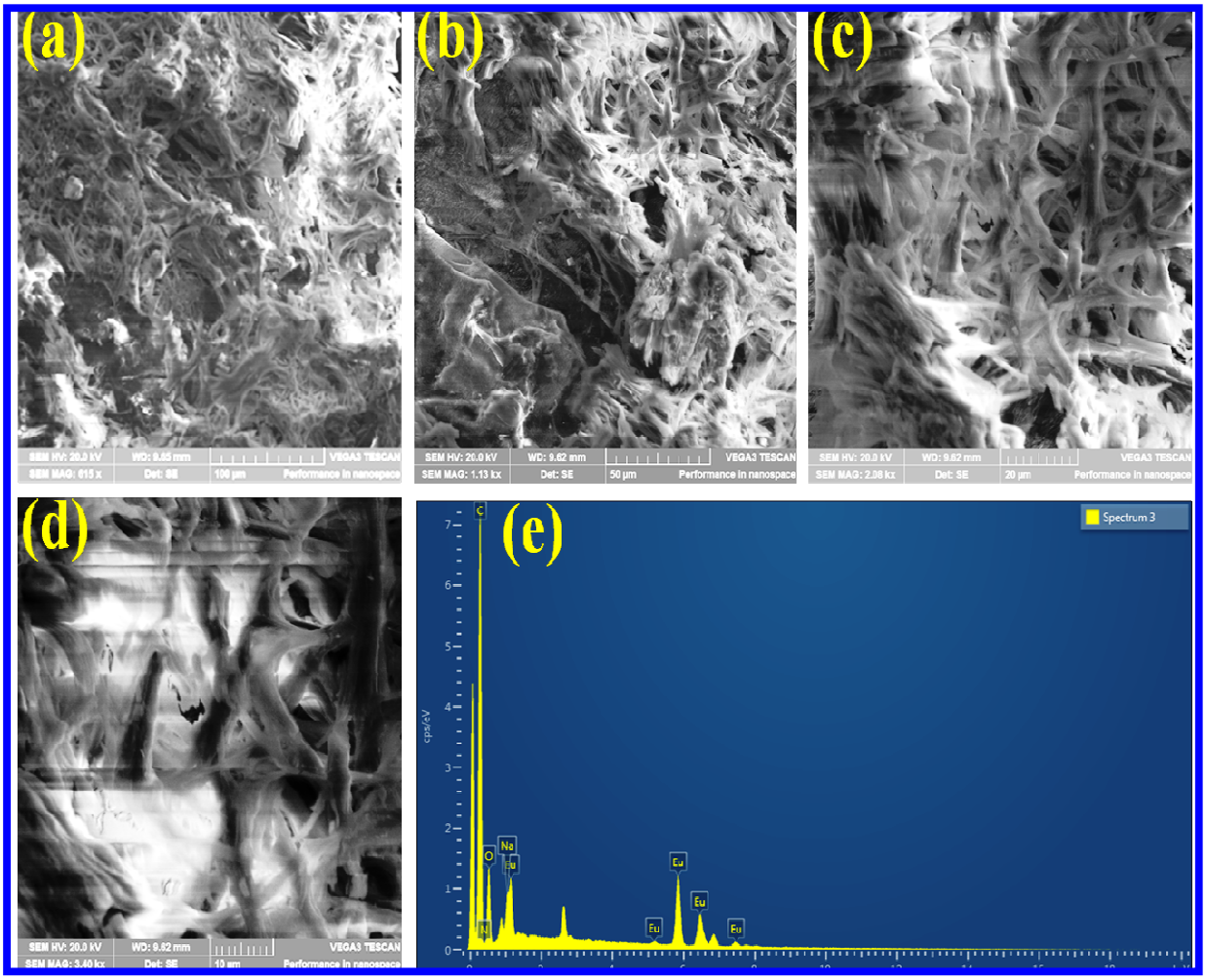

Fig.4A (a-e) SEM images of Eu(III)-CPLx with different magnification of (a) 100 µm, (b) 50 µm, (c) 20 µm ,(d) 10 µm and (e) EDAX analysis.

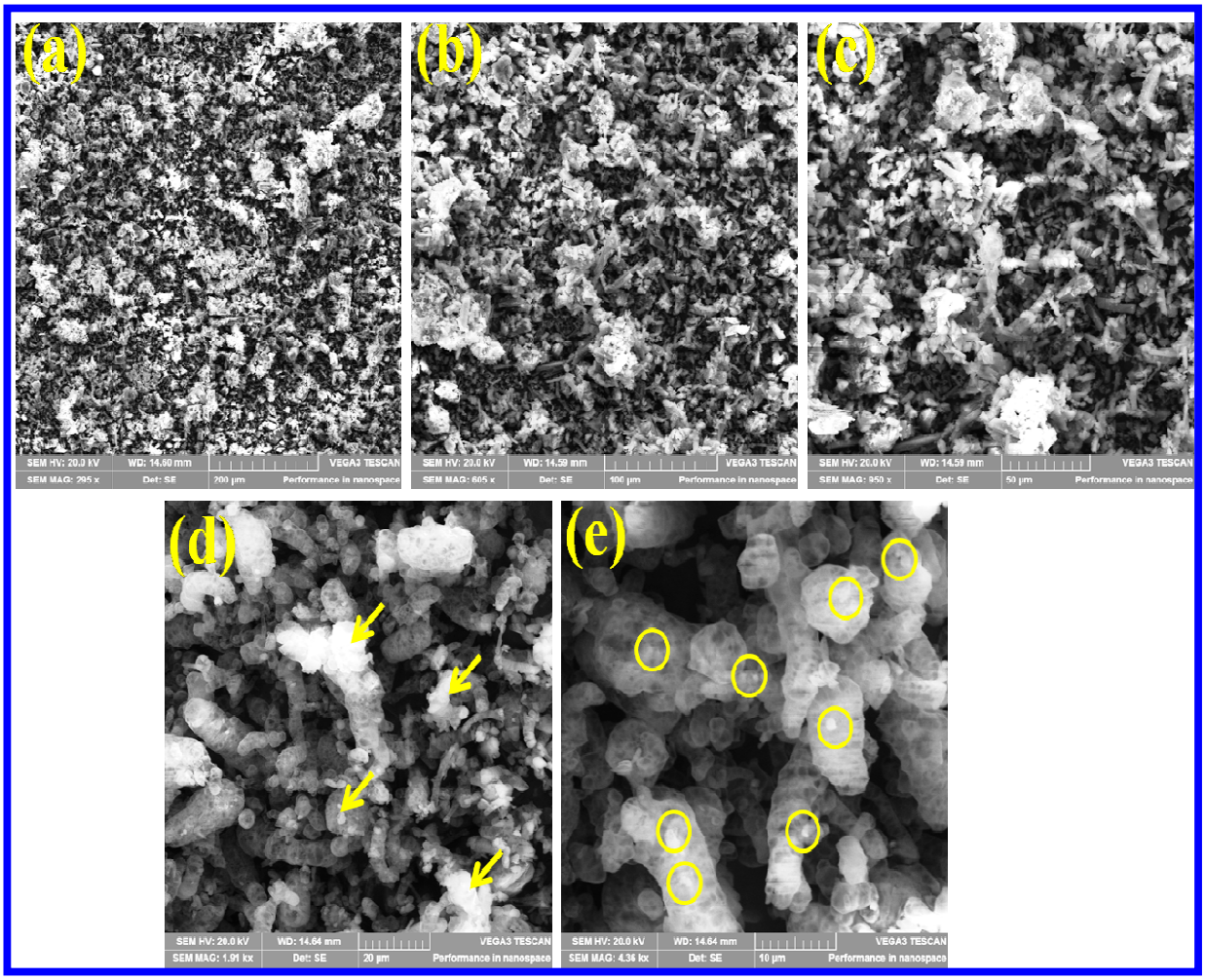

Fig.4B (a-e) SEM images of fluorescent Eu(III)-CPLx/D-Dex composite with different magnification of (a) 200 µM, (b) 100 µM, (c) 50 µM ,(d) 20 µM and (e) 10 µM.

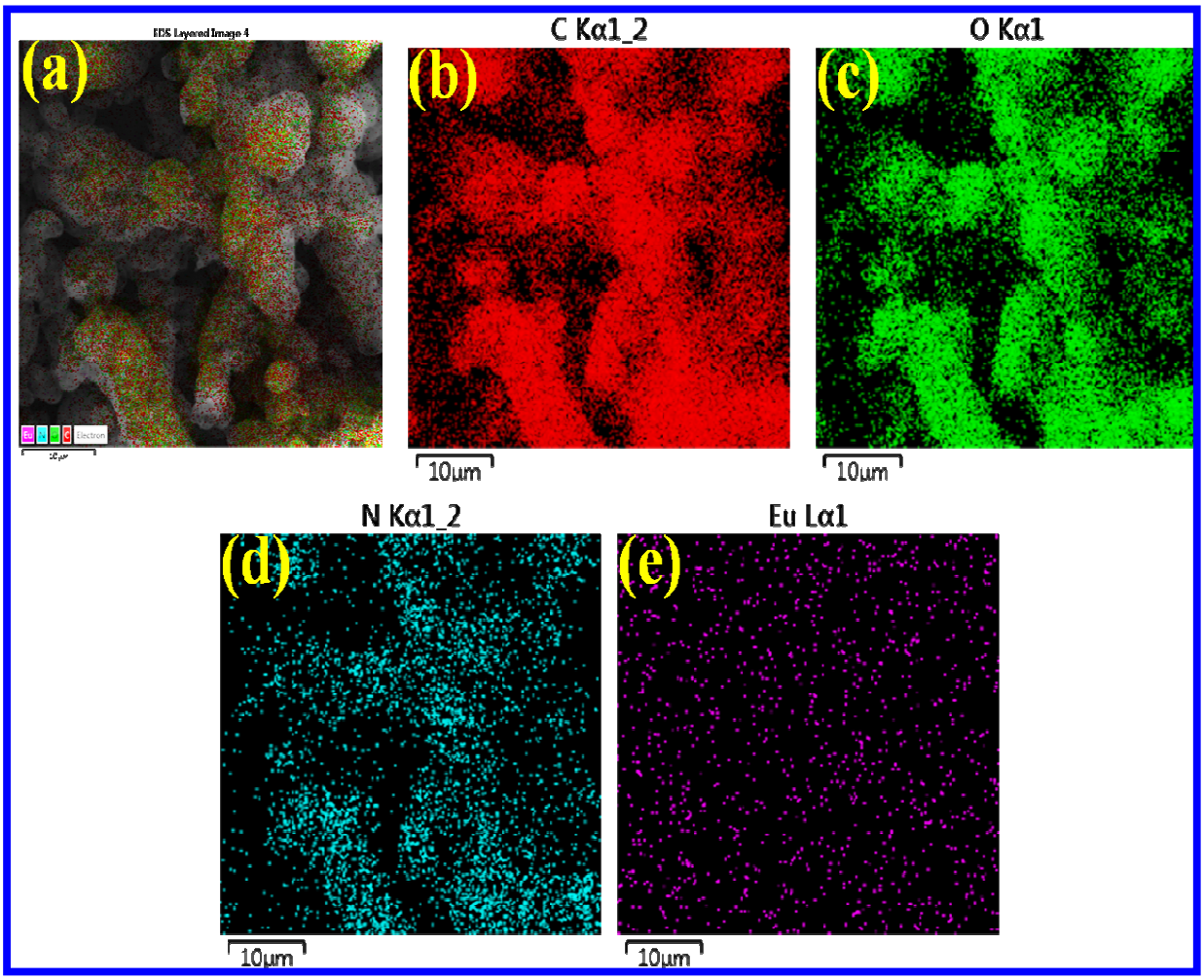

Fig.4C(a-e) Elemental mapping of fluorescent Eu(III)-CPLx/D-Dex composite of (a) SEM image at 10 um, (b) C, (c) O (d) N (e) Eu.

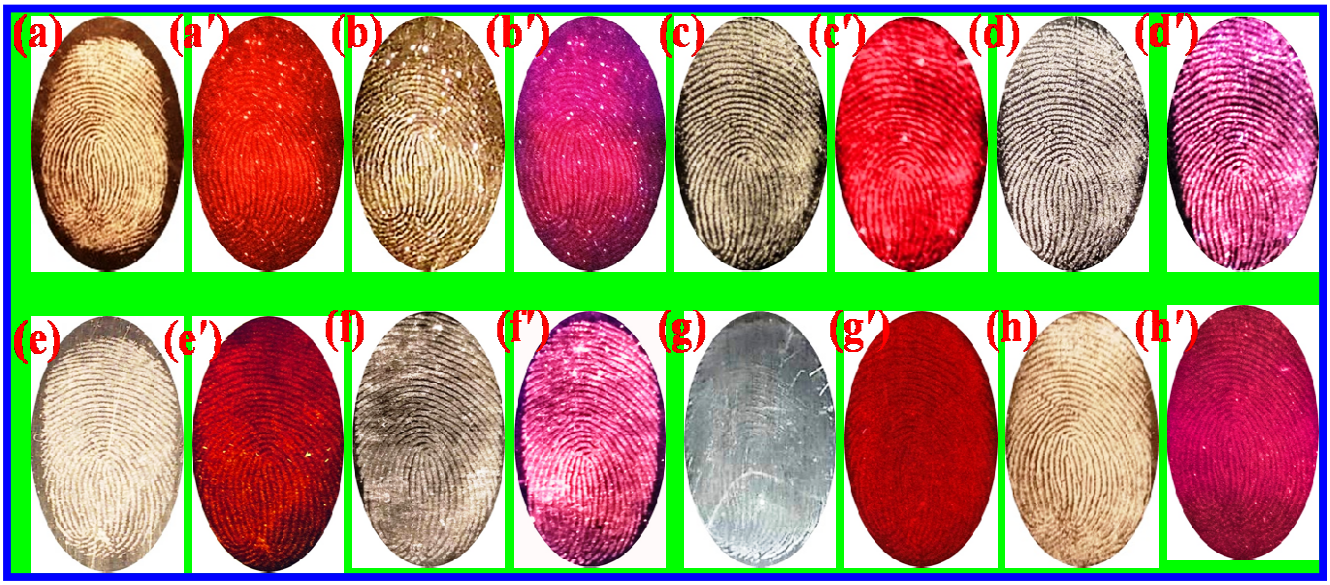

Fig.5 LFP images developed with Eu(III)-CPLx on (a, a′) glass slide, (c, c′) aluminum foil, (e, e′) aluminum sheet (g, g′) aluminum rod under day light and UV light at 365 nm and LFP images developed with fluorescent Eu(III)-CPLx/D-Dex composite on (b, b′) glass slide, (d, d′) aluminum foil, (f, f′) aluminum sheet (h,h′) aluminum rod under day light and UV light at 365 nm.

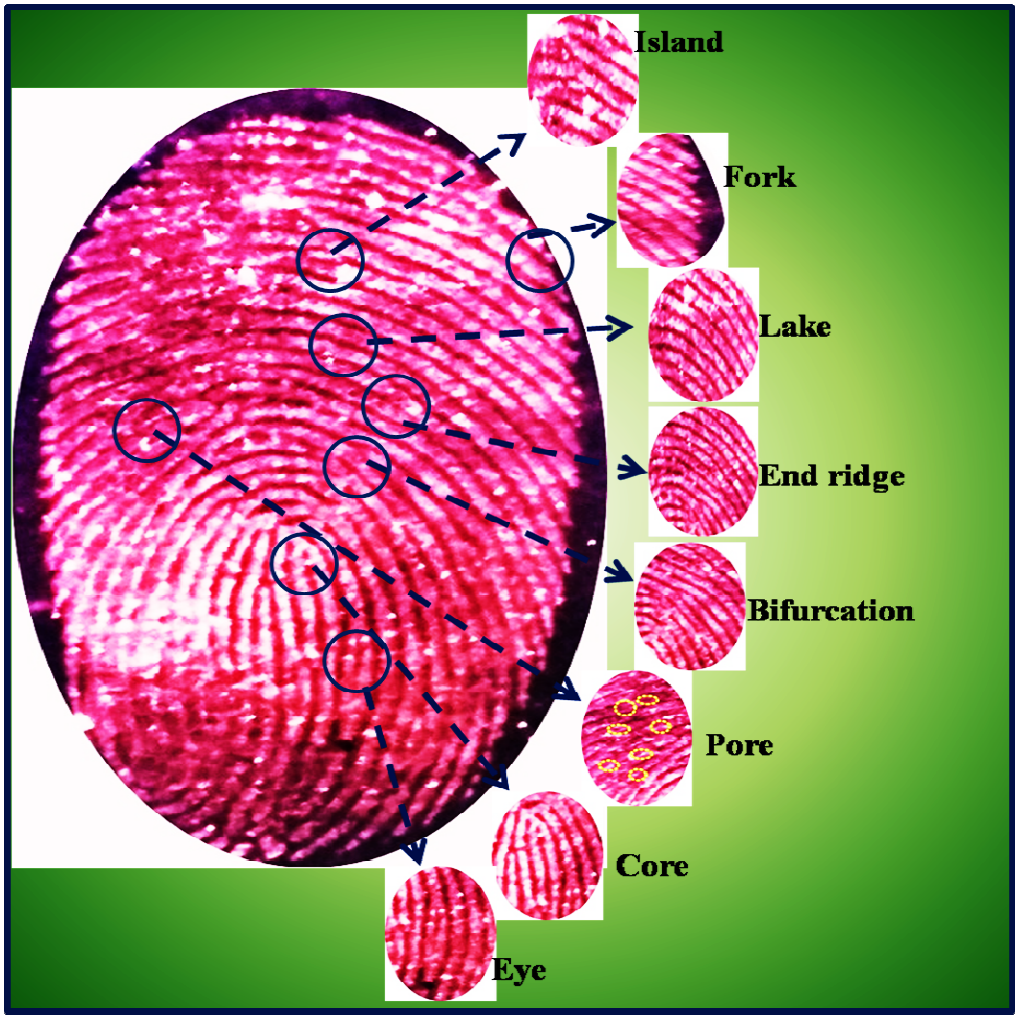

Fig.6 LFP images ridge details after developing on aluminum sheet substrate with fluorescent Eu(III)-CPLx/D-Dex composite including island, Fork, Lake, End ridge, Bifurcation, Pore, core and Eye under UV light irradiation at 365 nm.

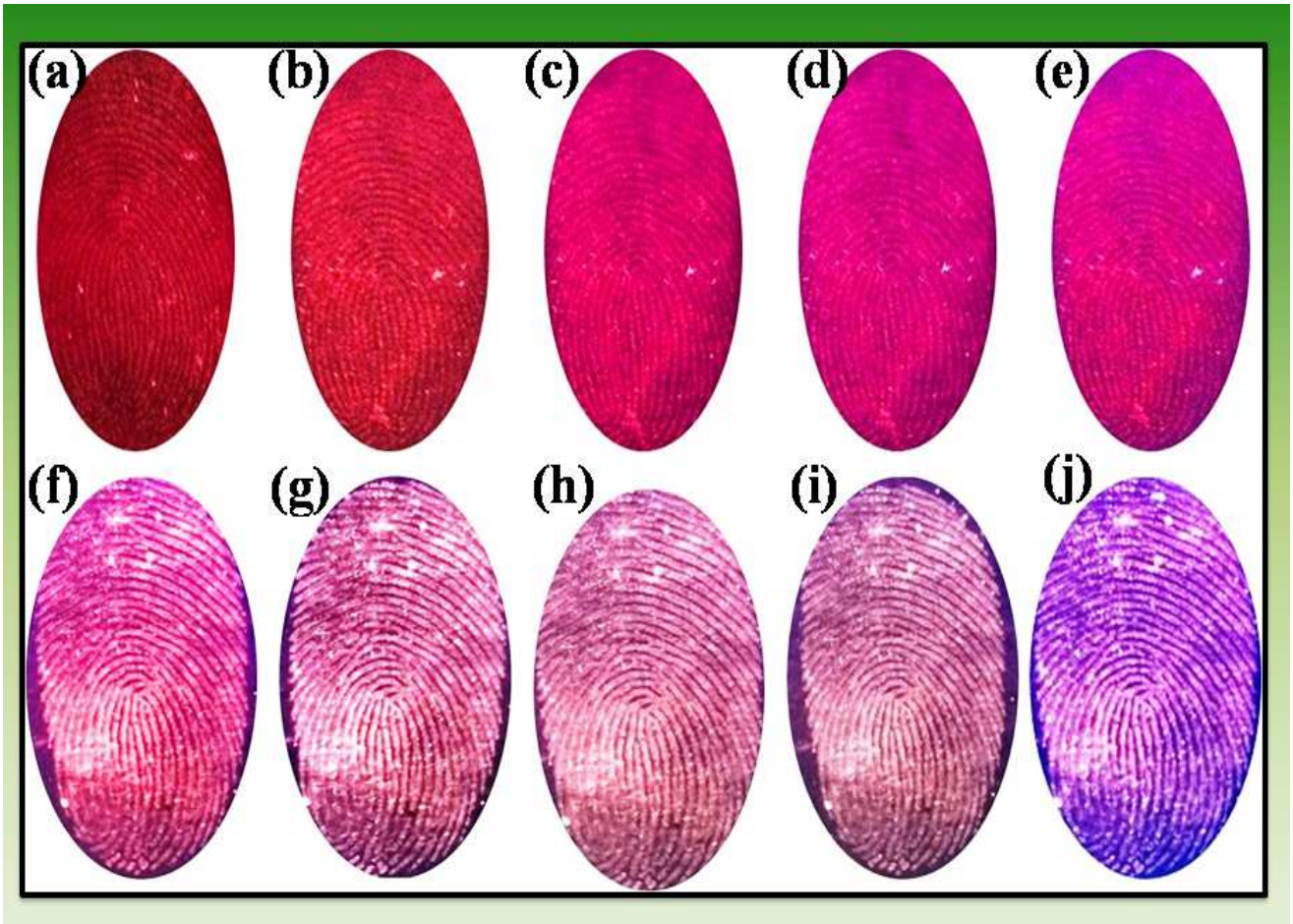

Fig.7(a-j) LFP developed on aluminum sheet with Eu(III)-CPLx different aging (a) 0 day, (b) 1 week, (c) 2 week, (d) 3 week and (e) 4 week under UV light light irradiation at 365 nm and LFP developed on aluminum sheet with fluorescent Eu(III)-CPLx/D-Dex composite different aging (a) 0 day, (b) 1 week, (c) 2 week, (d) 3 week and (e) 4 week under UV light light irradiation at 365 nm.

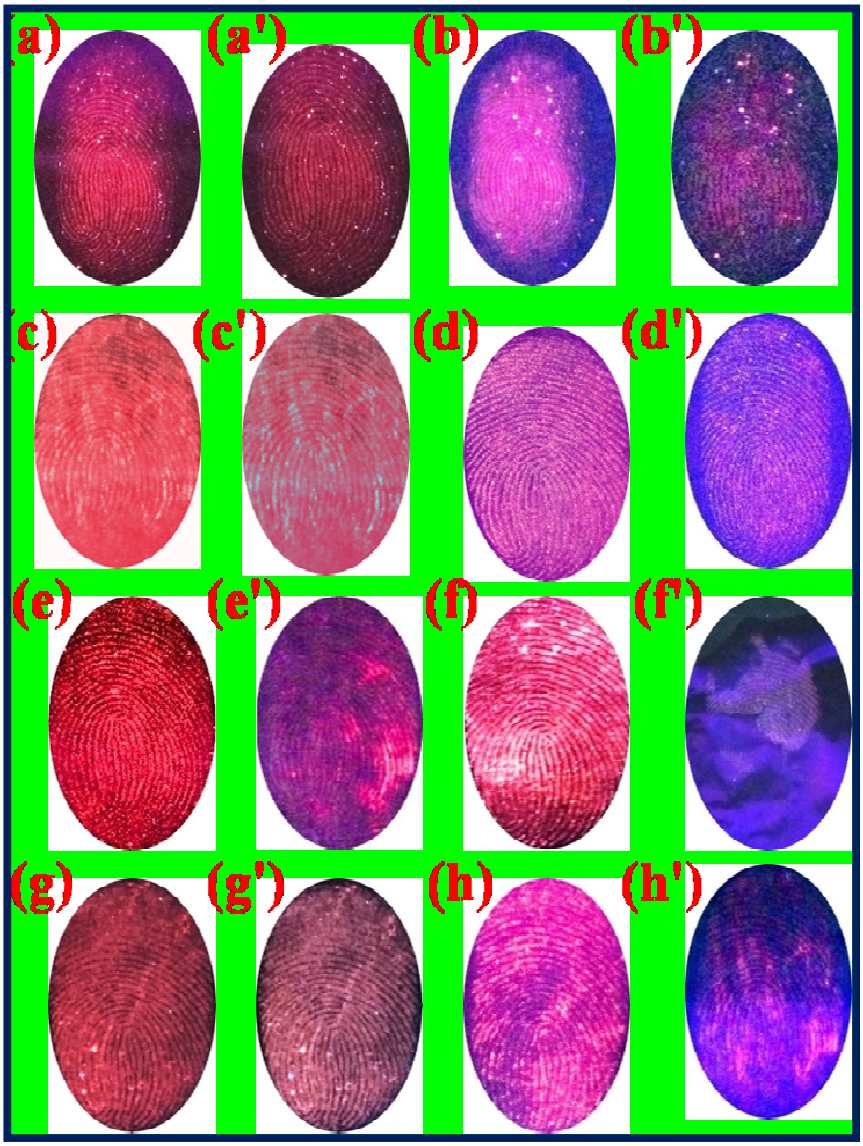

Fig.8 LFP images developed by before and after abrasion on different substrates with Eu(III)-CPLx (a, a′) glass slide, (c, c′) aluminum foil, (e, e′) aluminum sheet (g, g′) aluminum rod under day light and UV light at 365 nm and LFP images developed by before and after abrasion on different substrates with fluorescent Eu(III)-CPLx/D-Dex composite on (b, b′) glass slide, (d, d′) aluminum foil, (f, f′) aluminum sheet (h,h′) aluminum rod under day light and UV light at 365 nm.

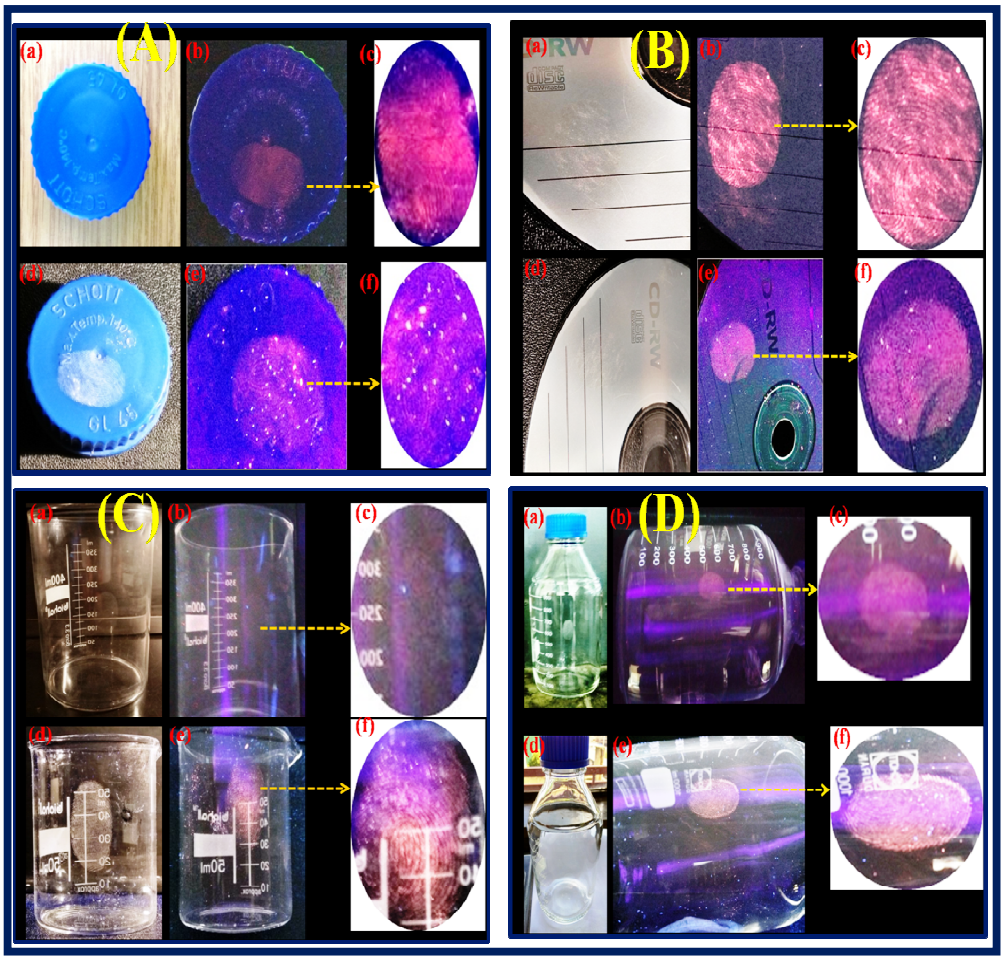

Fig.9(A-D) LFP detection different substrates with Eu(III)-CPLx and fluorescent Eu(III)-CPLx/D-Dex composite (A) (a, b)(d, e) plastic bottle lid (B) (a, b) (d, e) compact disc (C) (a, b)(d, e) glass beaker and (D) (a, b)(d, e) glass bottle under day light and UV-light irradiation at 365 nm. Expansion LFP image of (A) (c, f), plastic bottle lid (B) (c, f), compact disc (C) (c, f), glass beaker and (D) (c,f) glass bottle with Eu(III)-CPLx and fluorescent Eu(III)-CPLx/D-Dex composite under UV-light irradiation of 365 nm.

Fig

LFP images developed with Eu(III)-CPLx powder on South Africa currency (a,b) under the normal light and 365 nm UV light irradiation and (c) expanded LFP image, LFP images developed with fluorescent Eu(III)-CPLx/D-Dex composite on South Africa currency under the day light and 365 nm UV irradiation and (f) expanded LFP image.

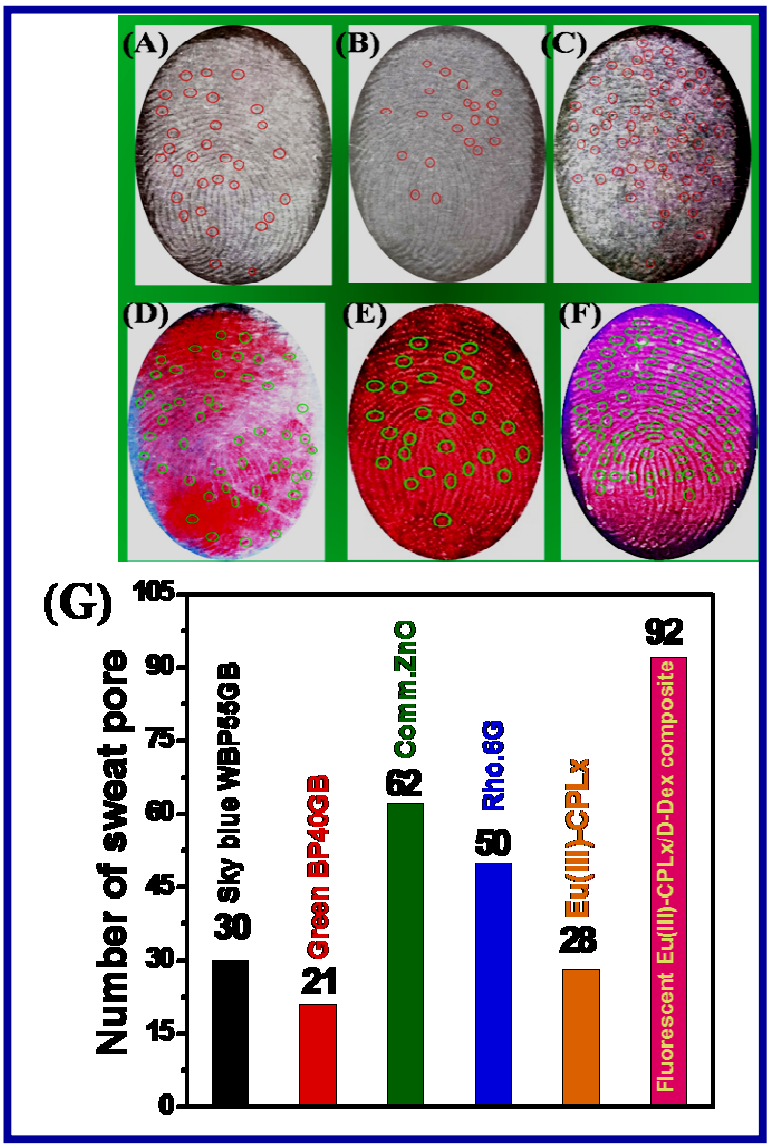

Fig.11(A-G) Comparison performance of LFP sweat pores by different labeling agents: (A) sky blue WBP 55G, (B) green BP 40G, (C) commercial ZnO powder, (D) Rhodamine 6G with day light, (E) Eu(III)-CPLx and (F) Fluorescent Eu(III)-CPLx/Dex composite under the UV light irradiation at 365 nm, (G) Calculate summarizing sweat pore.

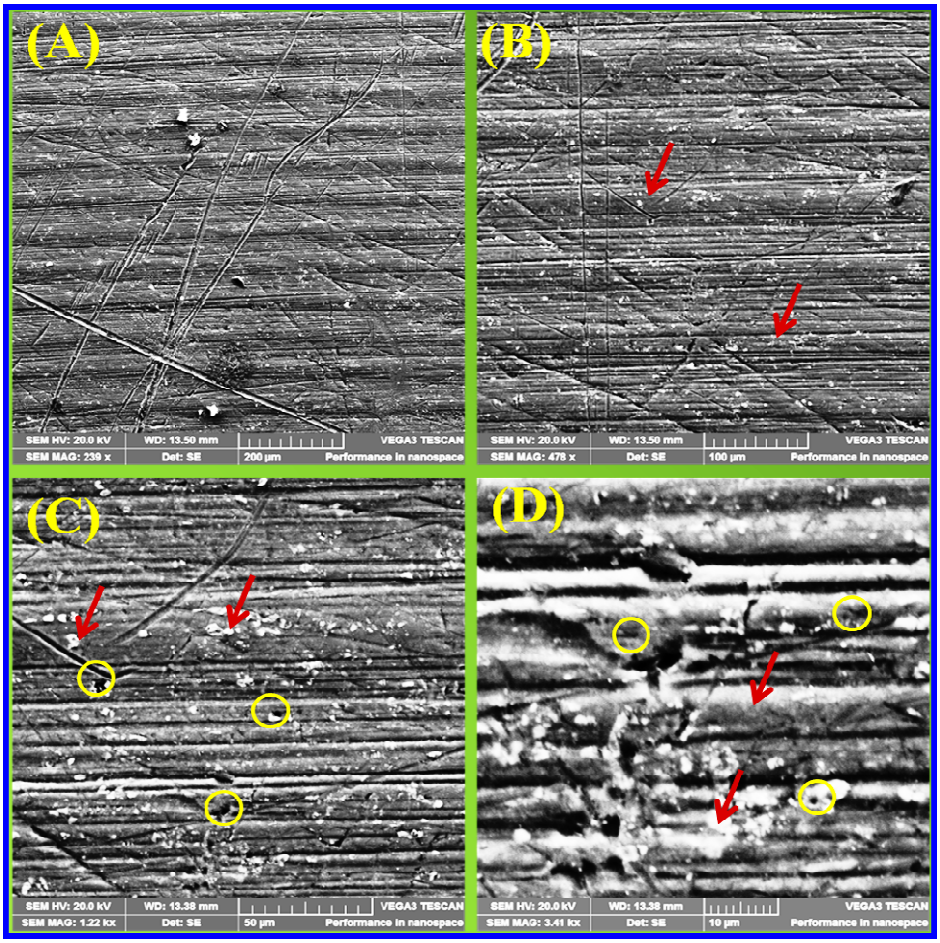

Fig.12 (A-D) SEM images of LFP detection on aluminum sheet with Eu(III)-CPLx (A) 200 µM (B) 100 µM, (C) 50 µM and (D) 10 µM.

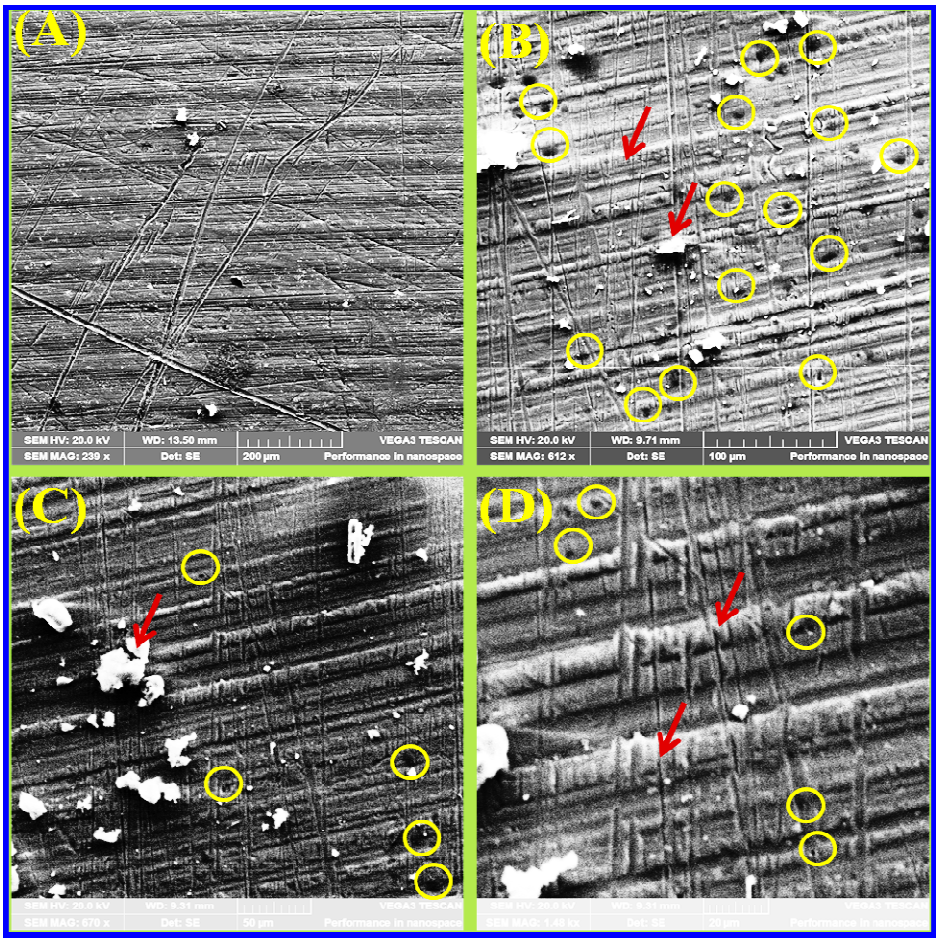

Fig.13 (A-D) SEM images of LFP detection on aluminum sheet with fluorescent Eu(III)-CPLx composite (A) 200 µM (B) 100 µM, (C) 50 µM and (D) 10 µM.

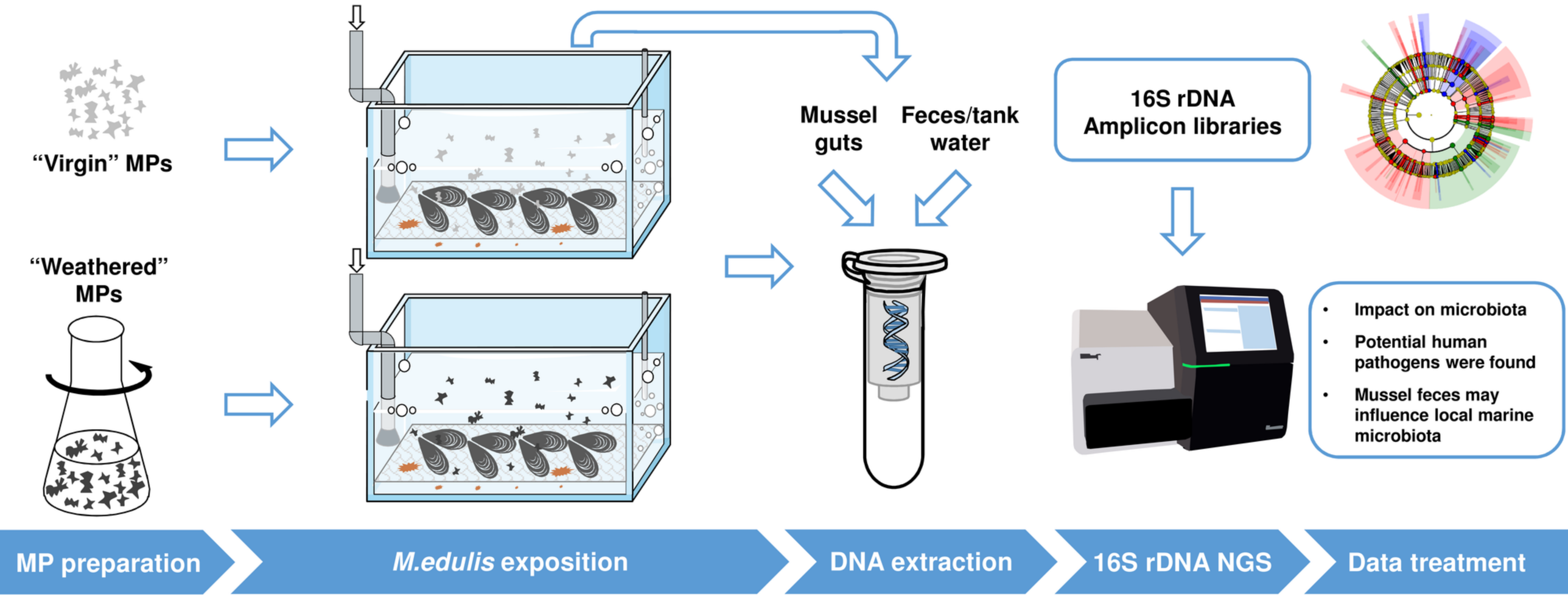
"Virgin" MPs
"Weathered" MPs
Mussel guts
Feces/tank water
16S rDNA Amplicon libraries
• Impact on microbiota
• Potential human pathogens were found
• Mussel feces may influence local marine microbiota
MP preparation
M.edulis exposition
DNA extraction
16S rDNA NGS
Data treatment